Available online at www.sciencedirect.com
SCIENCE DIRECT®
Journal of Human Evolution 47 (2004) 453–478

Comparison of inverse-dynamics musculo-skeletal models of AL 288-1 *Australopithecus afarensis* and KNM-WT 15000 *Homo ergaster* to modern humans, with implications for the evolution of bipedalism

Weijie Wang[a,b,*], Robin H. Crompton[a], Tanya S. Carey[c], Michael M. Günther[a], Yu Li[a], Russell Savage[a], Williams I. Sellers[d]

[a]*Department of Human Anatomy and Cell Biology, The University of Liverpool, Liverpool L69 3BX, U.K.*
[b]*Institute of Motion Analysis and Research, Department of Orthopaedics and Trauma Surgery, Ninewells Medical School, The University of Dundee, DD1 9SY, U.K.*
[c]*Equine Department, Warkwickshire College, Warwick CV35 9BL, U.K.*
[d]*Department of Human Sciences, Loughborough University, Loughborough LE11 3TU, U.K.*

Received 14 July 2003; accepted 28 August 2004

Abstract

Size and proportions of the postcranial skeleton differ markedly between *Australopithecus afarensis* and *Homo ergaster*, and between the latter and modern *Homo sapiens*. This study uses computer simulations of gait in models derived from the best-known skeletons of these species (AL 288-1, *Australopithecus afarensis*, 3.18 million year ago) and KNM-WT 15000 (*Homo ergaster*, 1.5-1.8 million year ago) compared to models of adult human males and females, to estimate the required muscle power during bipedal walking, and to compare this with those in modern humans. Skeletal measurements were carried out on a cast of KNM-WT 15000, but for AL 288-1 were taken from the literature. Muscle attachments were applied to the models based on their position relative to the bone in modern humans. Joint motions and moments from experiments on human walking were input into the models to calculate muscle stress and power. The models were tested in erect walking and 'bent-hip bent-knee' gait. Calculated muscle forces were verified against EMG activity phases from experimental data, with reference to reasonable activation/force delays. Calculated muscle

* Address for correspondence: Wang, W.J. Ph.D, Institute of Motion Analysis and Research, Department of Orthopaedics and Trauma Surgery, Ninewells Medical School, The University of Dundee, Dundee DD1 9SY, United Kingdom. Tel: +44 1382 660111 ext 34021; fax: +44 1382 496347.

E-mail addresses: w.wang@dundee.ac.uk (W. Wang), rhcromp@liv.ac.uk (R.H. Crompton), tcarey@warkscol.ac.uk (T.S. Carey), michaelg@liv.ac.uk (M.M. Günther), yu.li@bristol.ac.uk (Y. Li), rsavage@liv.ac.uk (R. Savage), w.i.sellers@loughborough.ac.uk (W.I. Sellers).

0047-2484/$ - see front matter
doi:10.1016/j.jhevol.2004.08.007

powers are reasonably comparable to experimentally derived metabolic values from the literature, given likely values for muscle efficiency. The results show that: 1) if evaluated by the power expenditure per unit of mass (W/kg) in walking, AL 288-1 and KNM-WT 15000 would need similar power to modern humans; however, 2) with distance-specific parameters as the criteria, AL 288-1 would require to expend relatively more muscle power ($W/kg.m^{-1}$) in comparison to modern humans. The results imply that in the evolution of bipedalism, body proportions, for example those of KNM-WT 15000, may have evolved to obtain an effective application of muscle power to bipedal walking over a long distance, or at high speed.

Keywords: Early hominid; Evolution of bipedalism; Musculoskeletal modelling; Force; Power

Introduction

The best known specimen of *Australopithecus afarensis*, AL 288-1 ('Lucy', 3.18 million year ago, or MYA) from the Hadar region of Ethiopia (Kimbel et al., 1994; Johanson et al., 1982) has a 40% complete skeleton. The stature is estimated at around 1.05 m and the weight at 30 kg (Jungers, 1982) so that stature is less, but build more robust than that of modern human adults (and children: for example, an 8-year-old female child in our study sample weighed 27 kg but her stature was 1.3 m). AL 288-1's lower limbs are short relative to the trunk and arms. KNM-WT 15000, the Nariokotome youth of *Homo ergaster*, 1.5-1.8 MYA (Brown et al., 1985) has a 75% complete skeleton, stature estimated at 1.45-1.6 m, weight 45-50 kg and in general has 'leggy' body proportions similar to those of modern teenagers. How would these distinctions in body proportions be reflected in distinctions in gaits? Would the distinctions in gaits help us to extend the great increase in ranging distances evidenced in the archaeological record from the period of *Australopithecus* to that of early African *Homo?*

While most would agree that any ape, including ourselves as well as early hominids, should be capable of a varied positional repertoire, including bipedalism, quadrupedalism and climbing (Rose 1991), it is highly unlikely that any hominoid could perform each of these biomechanically different modes of locomotion to equal levels of performance.

Knowledge of performance capabilities requires understanding of muscle action. Mechanical and electrical activity of muscles have been investigated by many authors in humans (e.g. Basmajian, 1974) and the time sequence of muscle activity during human walking has been particularly extensively investigated (e.g. Winter, 1991). Of all studies of the mechanics of muscles, the most influential remain the modeling and physiological studies of Hill (1938 and 1950). The Hill model describes muscle in terms of elastic and contractile elements. Direct measurement of muscle contraction and force within the body would be impractical in primates, and particularly so in great apes. While direct measurement has been performed by various workers on birds and some domestic mammals such as laboratory rats and sheep (e.g., Gillis and Biewener 2002), the relevance of such studies to primates must be questionable, in view of the phylogenetic distance, and verification against data from intact animals will inevitably be problematic.

It can reasonably be assumed that any species numerous enough to be represented in the fossil record must be, or have been, a successful one, and this implies that their anatomy is well adapted for their ecological niche. Normally, therefore, we reconstruct behaviour of fossil species by analogizing, identifying parallels in morphology and interpreting these in terms of the behaviour of living species. We cannot do so for the locomotor system of human ancestors, since we are the only living exemplar of an habitual biped. The unique combination of morphological features expressed in the skeleton of AL 288-1 and other australopithecines thus reflects a quantitatively unique positional repertoire (see, eg. Kimura et al., 1979; Prost, 1980; Lovejoy, 1981; Stern and Susman,

1983; Wolpoff, 1983; Susman et al., 1984; and review by Ward, 2002). The traditional analogizing approach to reconstructing the behaviour of extinct species is thus made difficult, if not impossible, as decades of disagreement over the locomotor repertoire of AL 288-1 and other australopithecines have made clear. The task is made no easier by the fact that at least in humans, the range of joint motion which occurs in bipedal walking is well below the physiological range of the joints involved, so that joint morphology of fossil specimens is somewhat less helpful than one might expect it to be, even supposing a close relationship between bony and cartilaginous joint form. However, it has long been clear that that there is a close relationship between locomotor behaviour and proportions of body segments, a relationship which has much to do with the simple mechanics of lever arms (Oxnard et al., 1989; Webb, 1996; Wang and Crompton, 2003). Bone proportions should thus be capable of indicating some information on the behaviour of fossil species. If we know the mass and mass distribution of body segments, and either the motion of these segments or the forces applied to them, we can calculate either unknown force or unknown motion capabilities. We do not, of course, know them for extinct species: but since we can measure external forces, body motion, inertial properties and body proportions in living species, and calculate missing parameters, we can model the consequences of alternative hypotheses in 'what-if' experiments. The currently available technique for prediction of internal forces or kinematics is simulation by dynamic modeling.

Since the 1970's, many authors have tried different approaches to solve multi-muscle dynamic modeling problems, which approaches may be divided into two kinds: 1) inverse dynamics approaches, where muscle forces are estimated from given external kinematic and kinetic data (e.g. Seireg and Arvikar, 1973; Hatze, 1977; Hardt, 1978; Pedotti et al., 1978; Crowninshield and Brand 1981; Patriarco et al., 1981); and 2) forward dynamics approaches, where muscle activity is input, and external kinematic and kinetic responses obtained (Hof and Berg, 1981; Olney and Winter, 1985; Neptune et al., 2001; Hase and Yamazaki, 2002). Neither technique is flawless: both require verification against real world data for living animals. But while a model is only as good as its assumptions, given enough computer power, assumptions can be changed as often as required and the consequences examined. For species with a long life-cycle, such as primates, no other method has this capability. Forwards dynamics is probably the ideal technique for studies of adaptation, because it can be used to generate various set of kinematics subject to the required criteria. In other words, there is no restriction on gaits which may be examined to those which currently exist, or may be artificially generated.

However, when the latter method is applied, the activity of many muscles has to be taken into consideration, extensive morphological physiological data is required, and solutions require very substantial computing time. This paper therefore applies the former, inverse-dynamics approach to a simple, 2D analysis of the musculo-skeletal structure of early hominids, applying human-like or ape-like kinematics to models, with the end of determining the forces and mechanical costs required for the models to perform bipedal walking. We are not ultimately concerned to predict which particular patterns of muscle activation early human ancestors might have used (several equally effective alternative patterns would exist), nor the absolute values of force and power requirements (the model does not take all aspects of muscle physiology and function into consideration) but simply what the relative scale of power and force requirements are for human-like walking over short and long distances, given differences in segment proportions between modern humans, AL 288-1 and KNM-WT 15000. Our study was conceived as an exploratory one. It would be hypothesized that no substantial differences in power requirements would be engendered simply by differences in body proportions, given human-like motion and relative muscle attachments. We also consider in part the effects of varying parameters such as inertial properties (body builds), muscle attachments and individual features such as tibia length. We have also considered different performance criteria (Crompton et al., 2003; Wang et al., 2003b) and presented an approach from

forward dynamics elsewhere (Sellers et al., 2003, 2004).

Materials and methods

Research path

The procedure of modelling is shown in Figure 1. The task consists of several stages: experiments on human walking (normal walking and 'bent-hip, bent-knee' or BHBK walking) are performed to collect joint motion and moments; bone dimensions are obtained by measurement or from the literature for the fossil skeletons and a modern human comparator; muscle attachments and physiological cross sectional areas (PCSAs) of modern humans or chimpanzee are applied, using a scaling approach, to the resulting models; the kinematics and moments are applied to the physical models in a simulation; then using mathematical optimization, muscle parameters, e.g. length, velocity and force, are estimated. If the simulated muscle force pattern is similar (given reasonable activation-force delays) to experimentally determined EMG patterns, the simulated muscle parameters are considered reasonably reliable; if not, rejected, and the simulation re-run with different settings; finally, calculated muscle power and stress are compared between subjects.

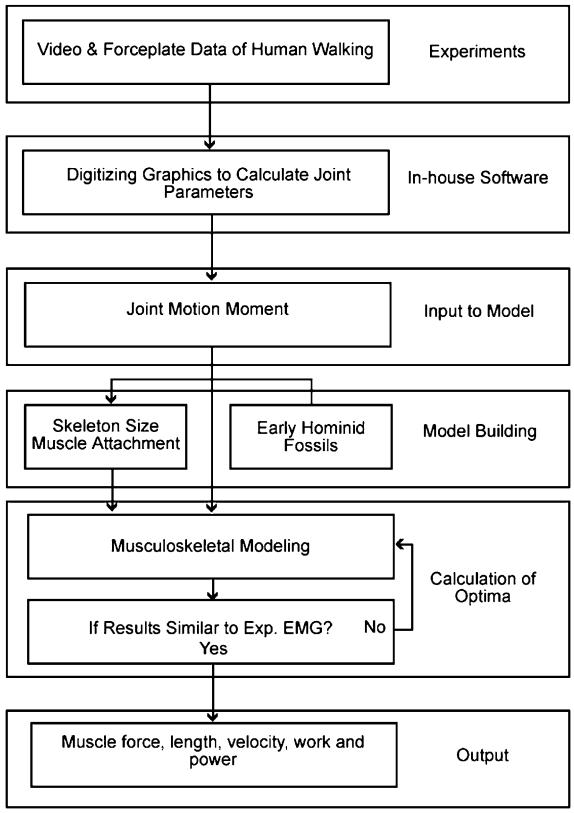

Fig. 1. Research flow chart. The task consists of several stages: Top three boxes: experiments on human walking are performed to collect joint motions and moments; and these joint motions and moments are applied, using a similar, scaling, approach to the models; Fourth box from top: bone dimensions are obtained by measurement or from the literature for the fossil skeletons, *right*, and *left*, a modern human comparator; muscle attachments and physiological cross sectional areas (PCSAs) of modern humans are applied, using a scaling approach, to the resulting models; Fifth box from top: *above*: simulations are run in our own dynamic modeling software and using mathematical optimization, muscle parameters, e.g. length, velocity and force, are estimated; and *below*: if the simulated muscle force pattern is similar (given known activation-force delays) to experimentally determined EMG patterns, the simulated muscle parameters are considered reasonably reliable; if not, rejected, and the simulation re-run with different settings; Bottom box: finally, calculated muscle parameters are compared between subjects.

Subject measurements

Subjects

The models of *Australopithecus afarensis* AL 288-1, *Homo ergaster* KNM-WT 15000 and male and female humans were constructed. Dimensions of the available and complete skeletal elements of AL 288-1 were obtainable from the literature (Johanson et al., 1982) as a cast was not available to us. Where bones are missing or incomplete, estimates were obtained from Jungers (1982) and Richmond et al. (2002). For KNM-WT 15000, measurements were made from a Kenya National Museum cast in our collection. Missing elements were scaled from measurements of human skeletons in our teaching collection. Markers were projected into the sagittal plane (e.g. with the anterior superior and anterior inferior iliac spines ASIS and AIIS projected so to lie in one plane), as our model is analysed in that plane. The dimensions measured on the model are illustrated in

Fig. 2A. The figure is purely illustrative, while actual landmarks are given in Table 1, and masses and leg lengths assigned listed in Table 2.

Methods for estimation of inertial properties in the fossil species, for measurement of physiological cross sectional areas (PCSAs) of muscle, for kinematic and kinetic measurements, and for calculation of moments from these are given in Wang (1999) and also in part in our previous papers (e.g., Crompton et al., 1996, 1998; Thorpe et al., 1998). All other methods follow Winter (1990, 1991) or are given below.

The length of the AL 288-1 tibia

According to indexes of limb proportions for *Homo sapiens, Pan troglodytes, Pan paniscus, Pongo pygmaeus*, and from complete elements of AL 288-1, KNM-WT 15000 and other early hominid skeletons (Richmond et al., 2002), humerus/femur length, humerus/femur circumference and radius/humerus length ratios are larger than those in *Homo* and KNM-WT 15000, but smaller than those of *Pan troglodytes* and *Pan paniscus*. Indices of AL 288-1 are closer to those in *Homo* than to those in *Pan troglodytes* and *Pan paniscus*. These indications suggest that the crural index (the ratio of the tibia to femur length) for AL 288-1 should fall between the crural indices of, on the one hand, *Homo* and on the other *Pan troglodytes* and *Pan paniscus*. From the same reference (Richmond et al., 2002), the crural index for *Homo* is about 83, about 83.5 for *Pan troglodytes* and 84 for *Pan paniscus*, and 88 for KNM-WT 15000. Considering that the higher crural index in KNM-WT 15000 might be influenced by climatic adaptations and a possible pathology (Richmond et al., 2002), we adopted 83.5 for the model of AL 288-1. Therefore, the tibia length was assumed to be 235 (cm) while the femur is taken to be 281 (cm), and the length of the two bones 516 (cm).

Muscles selected

Obviously, it is impossible to measure muscle properties of the fossils directly, and in many cases muscle markings on the available casts were indistinct. Instead, it is assumed not only that the muscle properties (i.e. physiological characteristics) of the fossil species were similar to those of modern humans, but also the muscle attachments. In humans, for example, rectus femoris originates from the anterior inferior iliac spine and inserts (via the patella) into the tuberosity of the tibia. In the fossils, the muscle attachments were regarded as having similar relative positions on the counterpart bones. Of course, the bone dimensions of the fossils decide where the muscle attachments are attached. Thus, each muscle for each subject has an unique 'geographical' location, which will influence the moment arm of muscles, and hence muscle force distributions.

When choosing muscles to model, we considered that each joint should be acted on by both single-joint and biarticular muscles, so that the effects of biarticular muscles could be taken into consideration. To simplify the modelling and reduce computational time, however, only nine main functional groups were considered: rectus femoris (RF), iliacus (IL), vastus lateralis and medialis (VS), the hamstrings with the exception of biceps femoris (short head): biceps femoris long head, semitendinosus, and semimembranosus (HA); separately, biceps femoris (short head) (BS), gastrocnemius (GA), gluteus (GU), tibialis anterior (TA) and soleus (SO) (see Fig. 2B). It is important to note that the simulated 'muscles' or 'muscle groups' used in this paper are simplified representations of the characteristics of several real muscles which in life contribute to each functional unit. The attachments are intended to represent those of the several real members of the muscle groups, and do not necessarily correspond to any actual individual muscle. The simulated 'muscle' groups produce the same motions in the sagittal plane for the hip, knee and talocrural (ankle) joints that apply to the muscle groups in real life: i.e., RF and IL as hip flexors, HA and GU as hip extensors, RF and VS as knee extensors, HA, GA and BS as knee flexors, GA and SO talocrural plantarflexors ('extensors'), and TA as talocrural dorsiflexor ('flexors').

A simplified representation of each major segment in the model lower limb skeleton (Fig. 2) was assembled, with the Anterior Superior and Anterior Inferior Iliac Spine positions on either side projected into the same sagittal plane so that the equivalent spines were superimposed. The femur on both sides rotates as a simple revolute joint in the

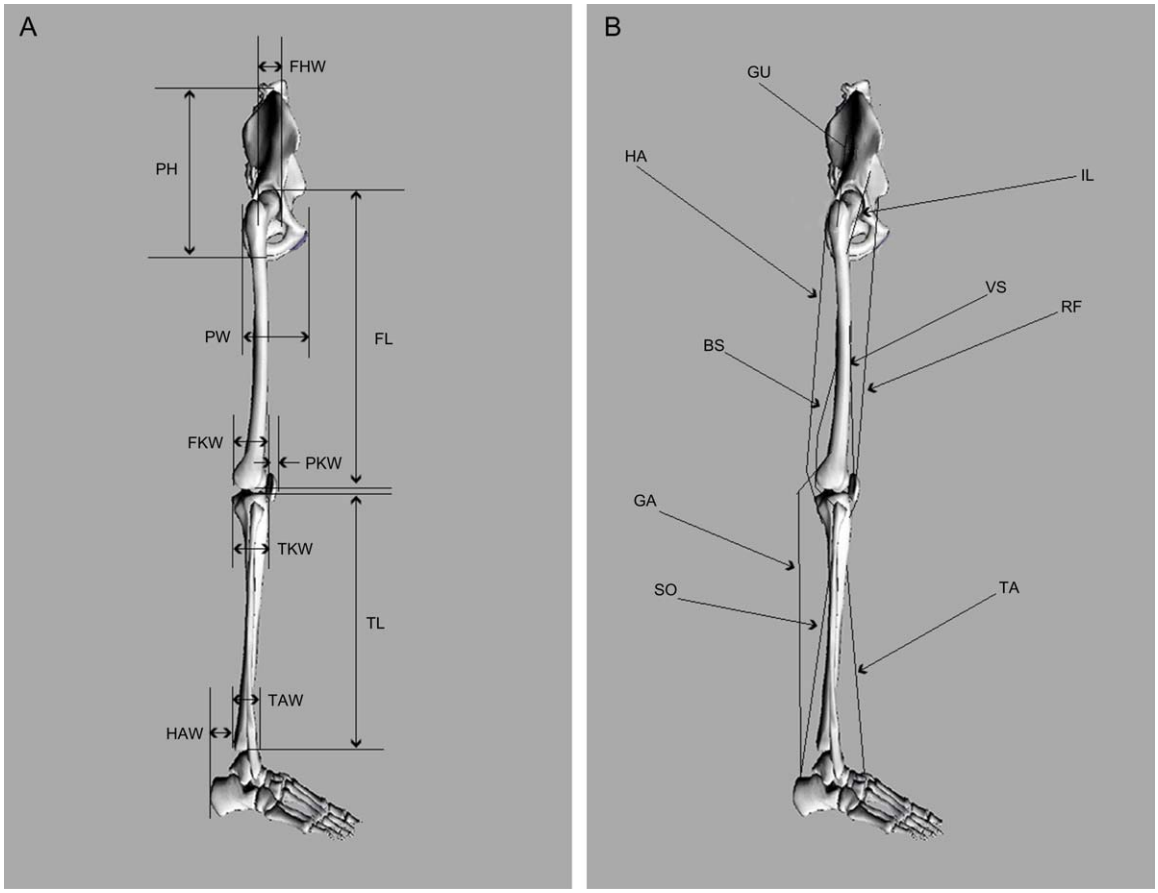

Fig. 2A. Measurements taken for fossil skeletons. Missing dimensions in the fossil specimens have been estimated by proportional scaling from the dimensions of modern humans. HAW: distance from most posterior point on margin of tibial malleolus to most posterior point on calcaneum when talocrural joint is articulated; PW: max. width of innominate; PH: max. height of innominate; FL: femur length, from most proximal point on greater trochanter to distalmost point on femur; FHW: width of femoral head; FKW: greatest anterioposterior dimension of femoral condyles; TL: tibia length; TKW: greatest anterioposterior dimension of tibial condyles; TAW: maximum anterioposterior dimension of tibial malleolus; and PKW: maximum anterioposterior dimension of patella.

Fig. 2B. 'Muscle' groups and their attachments on the musculoskeletal model

Name	Representing	Simplified Origin	Simplified Insertion
RF	Rectus femoris	Pelvis, AIIS	via patellar tendon into tibial tubercle
VS	Medial and lateral vasti	Anterolateral femoral shaft	via patellar tendon into tibial tubercle
TA	Tibialis anterior	Anteromedial tibia	medial cuneiform
GU	Gluteus maximus, Medius and minimus	External surface of ilium	Greater trochanter and gluteal tuberosity of femur
HA	Semimembranosus, Semitendinosus	Ischial Tuberosity	Proximal tibia (via *pes anserinus*)
GA	Gastrocnemius	Popliteal surface of femur	Calcaneal tuberosity
SO	Soleus	Soleal line on post. surface tibia and fibula	Calcaneal tuberosity
BS	Biceps femoris Short head	Posterior femoral shaft	Head of fibula
IL	Iliacus	Internal surface iliac blade	Lesser trochanter

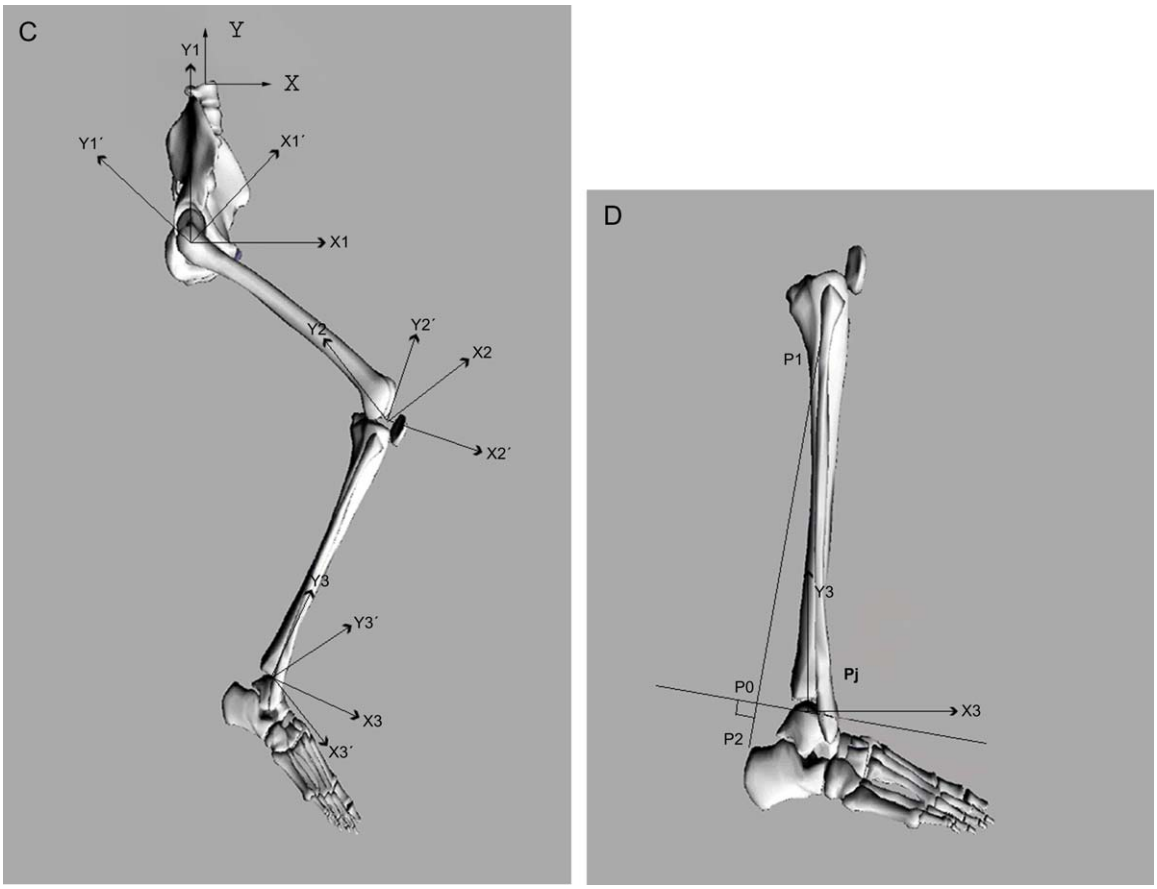

Fig. 2C. Diagram of the relationship between the proximal and distal local reference frames. Reference frames help us to calculate muscle parameters, such as length and moment arm. Muscle attachments are made relatively which means they maintain unchanged position on related bones. Use of local reference frames allows kinematics to be gathered and used as relative joint angles between adjacent segments. The coordinates of kinematics of more distal segments can be transferred into the parent, more proximal segments, and finally into the global reference for the whole model. Local reference frames: for the pelvis, femur and crus are fixed at the proximal end of each segment (the hip, knee, and ankle joints).

Fig. 2D. Illustration of variables required in calculations of moment arms of muscles (the section 4.3 in Materials and Methods). p_1 and p_2 are two points on a muscle, in this case the origin and insertion of soleus, and lie on a vector v_1 (p_1, p_2); p_0 marks the point representing the minimum perpendicular distance between this vector and the instant centre of the joint crossed (p_j), in this case the talocrural joint. Y3 and X3 represent the local reference frame of the tibia.

acetabulum. The knee and ankle joints were similarly represented as revolute joints projected into the same plane. Since this is not a 3D model, the pelvis did not tilt laterally and the 'bones' were assembled as 2D entities projected as they appear in Fig. 2, without medial or lateral rotation about their long axes. The foot was represented as a single unit. Table 3 gives the local coordinates of origin and insertion of each muscle, which can be used together with the bone data to give the proportional position of each attachment, and together with the reference frames, body mass and mass distribution data allow duplication of the inertial models we use. The muscle attachments on 'bones' were in the same proportional position in relation to both the length and width of the bones as they are in humans. Note that though the muscles in Table 3 are shown with two attachments (originations and insertions), muscles in reality wrap round joints no matter how a joint rotates. The wrapping radius is

Table 1
Skeleton size (cm) of fossil specimens and modern humans used for models

Subject	PW	PH	FL	FHW	FKW	TL	TKW	TAW	HAW	PKW
AL 288-1	8.53	17.47	28.1	2.7	2.4?	23.5*	3.1	2.4	2.6?	2.0?
KNM-WT 15000	11.5	20.1	42.8	4.4	5.8	34.8	4.8	3.7	3.0?	2.0?
Male1	11.0	19.0	42.0	4.3	6.0	35.0	4.5	3.5	3.25	2.0
Female1	10.5	19.0	41.0	4.0	5.5	35.5	5.0	3.5	3.0	2.0

Where HAW is distance from most posterior point on margin of tibial malleolus to most posterior point on calcaneum when talocrural joint is articulated; PW innominate max. width; PH innominate max. height; FL femur length from most distal point on greater trochanter to caudalmost point on femur; FHW femoral head width; FKW greatest anterioposterior dimension of femoral condyles; TL tibia length; TKW greatest anterioposterior dimension of tibial condyles; TAW maximum anterioposterior dimension of tibial malleolus; and PKW maximum anterioposterior dimension of patella width (see Fig. 2 for details).
Note: 1. AL 288-1 from Johanson et al. (1982); 2. KNM-WT 15000 data measured from the KNM-WT 15000 cast; 3. Male1 and Female1 skeletons, from the collection of the Department of Human Anatomy and cell Biology, The University of Liverpool. 4. Missing segments reconstructed by scaling from human values, and a sensitivity study will be applied. * Estimation of the tibia length of AL 288-1 is described in the text.

proportional to the bone width at the joint (e.g., the femoral head at the hip and the distal tibia at the talocrural joint). Wrapping avoids a possible simulation artifact, when the path of a muscle may penetrate a joint or segment.

Physiological cross-sectional area (PCSA)

We do not know the PCSAs of muscles in the fossil species, so to calculate muscle stress (defined by the ratio of the muscle force to PCSA), the PCSA of fossil specimens needs to be estimated. We can reasonably assume that PCSAs would have been within the range of variation of humans, on one side, and common chimpanzees, on the other, as the close relatives of the fossil species showing the most distinct locomotor behaviours. PCSA measurements for humans have been reported by Wickiewicz et al. (1983) and Friederich and Brand (1990) and for chimpanzees by Thorpe et al. (1999). We examined the effect of substituting human–like versus chimpanzee-like PCSA proportions into the AL 288-1 model as part of sensitivity testing, reported below.

To estimate muscle PCSA for fossil specimens, scaling was applied. If the most economic hypothesis, geometric similarity (McMahon, 1984), is assumed between fossil specimens and measurable subjects (such as modern humans), the PCSA of the model of a fossil should be proportional to the (2/3) power of the mass:

$$PCSA_{Mod} = PCSA_{MS}\left(\frac{Mass_{Mod}}{Mass_{MS}}\right)^{\frac{2}{3}} \quad (1)$$

Where subscript *'Mod'* is a model; *'MS'* a measurable subject; *Mass* the total body mass.

The scaled estimates of muscle PCSA are listed in Table 4. All muscle attachments are fixed on relative segments ('bones'), i.e., muscle attachments are defined in the relative, local, segment reference frame.

Biewener (1989) presents a case, based on the need for limbs to support body weight, for PCSA to scale to $Mass^{1}$: not $Mass^{2/3}$, but for the present purposes we regard two-thirds scaling (proposed by Alexander, 1985 based on maximum exerted forces) as more appropriate.

Table 2
The lower limb length and total weight of models

Model	AL 288-1	KNM-WT15000	Male1	Female1
Mass (kg)	30	49	66	55
Leg (m)	0.516	0.77	0.77	0.76

Experiments and the dynamic data needed for modelling

Experiments on human walking

A substantial number of experiments were done on human bipedal walking in different gaits, and abundant joint kinematic and kinetic data have been obtained therefrom by digization from standard 50 Hz video from two genlocked cameras and four 250 Hz digital video cameras, and most recently using a 6-camera, 1000Hz Qualisys

Table 3
Muscle attachments on bone (local coordinates) (m)

			AL 288-1			
Muscle	origin	x	y	insert	x	y
RF		0.050	−0.058		0.020	−0.023
VS		0.014	−0.094		0.020	−0.023
TA		0.016	−0.038		0.029	−0.029
GU		−0.040	−0.058		−0.039	−0.035
HA		−0.040	−0.175		−0.017	−0.029
GA		−0.017	−0.234		−0.038	−0.038
SO		−0.016	−0.077		−0.038	−0.038
BS		−0.017	−0.094		−0.016	−0.038
IL		0.050	−0.017		0.014	−0.028
			KNM-WT 15000			
Muscle	origin	x	y	insert	x	y
RF		0.065	−0.067		0.020	−0.035
VS		0.022	−0.143		0.020	−0.035
TA		0.024	−0.058		0.044	−0.044
GU		−0.050	−0.067		−0.049	−0.054
HA		−0.050	−0.201		−0.029	−0.044
GA		−0.029	−0.357		−0.049	−0.058
SO		−0.024	−0.116		−0.049	−0.058
BS		−0.029	−0.143		−0.024	−0.058
IL		0.065	−0.020		0.022	−0.043
			Female1			
Muscle	origin	x	y	insert	x	y
RF		0.065	−0.063		0.020	−0.036
VS		0.020	−0.137		0.020	−0.036
TA		0.025	−0.059		0.042	−0.044
GU		−0.048	−0.063		−0.048	−0.051
HA		−0.048	−0.190		−0.028	−0.044
GA		−0.028	−0.342		−0.048	−0.059
SO		−0.025	−0.118		−0.048	−0.059
BS		−0.028	−0.137		−0.025	−0.059
IL		0.065	−0.019		0.020	−0.041
			Male1			
Muscle	origin	x	y	insert	x	y
RF		0.055	−0.063		0.020	−0.035
VS		0.022	−0.140		0.020	−0.035
TA		0.022	−0.058		0.042	−0.044
GU		−0.040	−0.063		−0.039	−0.053
HA		−0.040	−0.190		−0.030	−0.044
GA		−0.030	−0.350		−0.050	−0.058
SO		−0.023	−0.117		−0.050	−0.058
BS		−0.030	−0.140		−0.023	−0.058
IL		0.055	−0.019		0.022	−0.042

Note:

Muscle	Simplified Origin Assigned	Via Joints Assigned	Simplified Insertion
RF	Pelvis, AIIS	Hip, knee	via patellar tendon into tibial tubercle
VS	Anterolateral femoral shaft	Knee	ibid
TA	Anteromedial tibia	Ankle	medial cuneiform
GU	External surface iliac blade	Hip	Gtr trochanter and gluteal tuberosity of femur
HA	Ischial tuberosity	Hip, knee	Proximal tibia (*pes anserinus*)

Table 3 (*continued*)

GA	Popliteal surface of femur	Knee, ankle	Calcaneal tuberosity
SO	Soleal line on post. surface tibia and fibula	Ankle	ibid
BS	Posterior femoral shaft	Knee	Head of fibula
IL	Internal surface iliac blade	Hip	Lesser trochanter of femur

motion capture system, but in each case obtaining synchronous kinetic data from a Kistler 9821B forceplate (see, e.g. Li et al., 1996, Wang et al., 1996 and 1998, and see Appendix). We calculated joint angles and moments at the hip, knee and ankle, using standard methods (see Winter, 1990) and on the basis video sequences and force platform data. Since joint motion is somewhat variable in different individuals, the averages of joint angles and moments from 6 subjects were applied to the calculations of the musculoskeletal models. These input data are given in Fig. A1 (joint angles) and Fig. A2 (joint moments) to allow duplication of our study, with the addition of the data for the models to which joint motions and moments were applied.

Normalisation of joint moments

Before inputting 'actual' joint moments to a model, joint moments obtained from experiments were transformed proportionally, using the following equation:

$$\frac{Moment_{Mod}}{Mass_{Mod}Leg_{Mod}} = \frac{Moment_{Sta}}{Mass_{Sta}Leg_{Sta}} \quad (2)$$

Where subscript "*Sta*" means the standard data from experiments, where the moments, masses and leg lengths are the average of 6 subjects; and subscript *"Mod"* model data (masses and lower limb lengths are listed in Table 1). Using Eq. (2), the joint moment to be applied to a model can be obtained. The moments are considered as the real "drivers" of joint motion for the models.

Since joint angles are dimensionless, they may be applied directly to the models.

Normalisation of speed

As the models have different statures, walking velocities should vary between models. For example, as AL 288-1 is shorter than other subjects,

Table 4
PCSA (cm^2) assigned to models

	Male[1]	Female[1]	AL 288-1(F)	KNM-WT15000	Male1	Female1	AL 288-1(C)
Muscle							
GU	20.20	10.76	7.55	10.48	12.78	11.32	24.26
IL	23.33	8.82	6.19	8.59	10.47	9.28	17.39
BF(L)	27.34	9.12	6.40	8.88	10.83	9.59	4.43
RF	42.96	9.20	6.46	8.96	10.92	9.68	9.83
Semim.	46.33	13.99	9.82	13.62	16.61	14.71	3.48
Semit.	23.27	3.12	2.19	3.04	3.71	3.28	3.13
BF(s)	8.14	4.69	3.29	4.57	5.57	4.93	4.00
VS(m)	66.87	15.60	10.95	15.19	18.53	16.41	8.70
GA(m)	50.60	17.00	11.93	16.55	20.19	17.88	9.22
TA	16.88	8.48	5.95	8.26	10.07	8.92	4.61
SO	186.69	57.72	40.52	56.20	68.55	60.70	19.13

Note:
1) [1] Friederich and Brand (1990); [2] Thorpe et al. (1999);
2) Model PCSA obtained on the basis of assuming geometric similarity: see Eq (1) in the text;
3) AL 288-1 (F): AL 288-1's PCSA normalized by using human female data [1];
4) AL 288-1 (C): AL 288-1's PCSA normalized by using chimpanzee data [2];
5) Other models normalized by using human female data [1] to compare with AL 288-1;
6) Muscle/muscle group names given in the text.

what is a normal speed for a human adult would be a fast one for AL 288-1. To apply an "equivalent" velocity, Alexander (1984, 1992) introduced the Froude number:

$$Froude = \frac{v^2}{gL} \tag{3}$$

where v is velocity (m/s), L leg length (m), and g gravitational constant (m/s^2). All equivalent velocities and durations for the different models are listed in Table 5. For example, while a modern human walks at a speed of 1.47 (m/s) and takes 1.07 (s) for a stride, AL 288-1 would walk at an equivalent speed of 1.18 (m/s) and take 0.86 (s).

Modelling

Local reference frames

To compute muscle force and power, some muscle parameters, including length, velocity and moment arm of muscles, must first be calculated. To do so, we have defined a global reference for the whole model, and local reference frames for each segment at the pelvis, hip, knee and ankle (see Fig. 2C). Using any two neighbouring frames, one fixed at the proximal segment and the other at the distal segment, the distal local coordinates can easily be transferred into the parent coordinates, and thence into the global coordinates. In this way, as the muscle attachments are made on 'relative' 'bone' segments, it is convenient to describe muscle kinematics as a joint rotates over a given relative angle.

Table 5
Equivalent velocity and duration time for all models

Gaits	Slow	Normal	Fast	BHBK
	Experimental velocity (m/s)			
Exp. Subj	1.0380	1.470	1.933	1.2261
Model	Equivalent velocity (m/s)			
AL 288-1	0.8296	1.1749	1.5449	0.9973
KNM-WT 15000	1.0184	1.4422	1.8964	–
Male1	1.0184	1.4422	1.8964	–
Female1	1.0117	1.4328	1.8841	–
	Experiment duration time (s)			
Exp. Subj.	1.2880	1.0720	0.9000	1.4680
Model	Equivalent duration time (s)			
AL 288-1	1.0294	0.8568	0.7193	1.1940
KNM-WT 15000	1.2636	1.0517	0.8830	–
Male1	1.2636	1.0517	0.8830	–
Female1	1.2554	1.0449	0.8772	–

Note: 1. Exp. Subj: experimental subjects; 2. Equivalent time or velocity: the values used in the simulations; BHBK: 'bent-hip bent-knee' gait.

The distal frame enables us to utilise relative joint angles between the adjacent segments, which are relatively easy to obtain in actual experiments on humans walking. In the distal frame, muscle attachments maintain unchanged position on related bones. The whole distal frame rotates about a joint centre in the proximal frame (see Fig. 2C). Under these conditions, the coordinates in the two frames have a relationship as follows:

$$\overline{v}_3 = \overline{v}_1 + R \cdot \overline{v}_2 \tag{4}$$

where v_1 and v_2 are the vectors of the muscle path in the proximal and distal reference frames respectively, v_3 is their total; and R is a rotation matrix:

$$R = \begin{bmatrix} \cos(\theta) & \sin(\theta) \\ -\sin(\theta) & \cos(\theta) \end{bmatrix} \tag{5}$$

where θ is a relative joint angle between the two neighbour reference frames.

Muscle length and velocity

If a muscle attachment on a frame (segment or bone) is defined, the attachment's coordinates related to the other reference frame can be calculated easily. Moreover, when the segment rotates, the muscle length, in either the proximal or the distal system, can be obtained.

For example, if a muscle, such as VS, originates from point p_1 on the femur, passes through point p_2 on the patella (which is assumed to be fixed on the tibia) and inserts on point p_3 on the tibia, the muscle length should be the sum of the distances from p_1 to p_2 and p_2 to p_3.

$$l_m = D(p_1, p_2) + D\left(p_{2,} R \cdot p_3\right) \tag{6}$$

where l_m is the muscle length; and D the distance between two points.

The method is very convenient in the calculation of muscle parameters. If the local coordinates of muscle attachment and the relative joint angles

are given, the length of a biarticular muscle can be calculated easily.

Once the muscle lengths at each instant during a sequence of walking are obtained, the muscle's contracting or stretching velocity can be calculated with:

$$v_m = -\frac{dl_m}{dt} \tag{7}$$

where l_m is muscle length (m), v_m muscle velocity (m/s) and dt time interval; the negative sign indicates that muscle velocity is assumed to be positive when the muscle contracts. That is, the concentric action of a muscle is defined as positive and the eccentric negative. Muscle displacement, velocity and force have similar sign definitions.

Moment arms of muscle

In this study, a simple method of calculating moment arm from joint position and muscle attachments was employed for simulations. If a muscle's local coordinates (attachments on bone) and the relative joint angle between two segments are given, the overall 'muscle fibre direction' (line of action) can be calculated. Thus, the moment arm of muscle about the joint can be derived. For example, there are two vectors $v_1(p_1, p_2)$ and $v_2(p_0, p_j)$ (see Fig. 2D). When the two vectors come to lie at right angles, their dot-product should be 0. In addition, p_0 must be on the same line as p_1 and p_2. Thus, there is a group of equations:

$$\begin{aligned} &v_1(p_1,p_2) \bullet v_2(p_j,p_0) = 0 \\ &L_l(p_0) = L_l(p_1) = L_l(p_2) \\ &a_m = D(p_j,p_0) \end{aligned} \tag{8}$$

where, p_1 and p_2 are two points on a muscle; p_j is the instant centre of the joint; p_0 is a point shared by vectors v_1 and v_2; L_l is a linear equation determined by p_1 and p_2; a_m the moment arm of muscle (m); v_1 a vector between two points on the muscle; v_2 a vector between p_0 and p_j. Generally, p_1, p_2 and p_j are given, then p_0 can be calculated using Eq. (8). Thus, the moment arm of the muscle can be obtained.

Calculation of muscle force

While muscle forces are undoubtedly responsible for producing joint moments to drive segment motion, it is less clear how muscles actually work together to produce these joint moments. As indicated in the Introduction, many have tried to solve the problem using optimisation approaches, and the present study takes a similar approach to those in the literature, building on their achievements. Presumably, in order to produce joint moments, the muscles around the joint optimally distribute their forces so that the total of muscle forces or the total of muscle powers reaches a minimum. In terms of mathematical optimisation, the problem can be expressed as follows.

$$\text{Minimum } \sqrt[m]{\sum_{i=1}^{n}\left(\frac{f_i(t)}{PCSA_i}\right)^m} \tag{9a}$$

$$\text{or : Minimum } \sum_{i=1}^{n}(|v_i(t)|f_i(t)) \tag{9b}$$

$$\text{Subject to } A \cdot F = M \tag{9c}$$

where $f_i\,(t)$ muscle force (N) in ith muscle at time t; $v_i\,(t)$ muscle velocity in ith muscle at time t; n the number of muscles; F a vector of muscle forces; A the matrix of moment-arm of muscles; M a vector of joint moments; $PCSA_i$ PCSA in ith muscle; m a power, 2 or 3 (see Crowninshield and Brand, 1981). In this study, there are nine muscles (groups) and three joints under consideration. Therefore, M in Eq. (9) includes the moments of force at the hip, knee and ankle. Matrix A includes the moment arms of the muscles about the three joints.

Equation (9) was solved by means of Linear Programming (Matlab®, 2002). To estimate a distribution of muscle forces using mathematical optimization, a variety of forms of objective functions are available in the literature. Pedotti et al. (1978) considered the minimum of the sum of all muscle force (divided by its maximum muscle force) as the objective function, while Hardt (1978) applied the minimum of the power, as in Eq. (9b). Crowninshield and Brand (1981) used the minimum of the sum of muscle forces (divided by its PCSA), the form seen in Eq. (9a), and the results obtained in this way showed closer agreement between the muscle force and experimental EMG patterns than previous methods. Glitsch and

Baumann (1997) extended Crowninshield and Brand (1981)'s method to multi-muscle situations in a semi-three-dimensional environment. In our own trials, it was observed that using equation (9a), the muscle force obtained is more similar to experimental EMG patterns than using equation (9b), and thus Equation (9a) was adopted for final calculations.

Muscle power

Physiologically, when a muscle contracts, it produces a force, and the contracting direction is defined as positive and the concentric force as positive force. A muscle cannot produce an eccentric force by itself. If a muscle is acted on by an eccentric force, that force should be produced by other muscles that are contracting, or applied by joint motion or by connective tissue. When a muscle force and its velocity have the same sign, positive power is produced, otherwise, negative power. Since both positive and negative muscle powers may consume chemical energy, muscle powers are calculated as below:

$$P = \sum_{i=1}^{n} \left(\frac{1}{N} \sum_{t=0}^{t\,\max} |f_i(t) \cdot v_{mi}(t)| \right) \tag{10}$$

where P is power (Watt); N the number of calculated frames; and other symbols are the same as those in Eq. (9).

Normalised power for comparisons

Since muscle power directly impacts on energy expenditure, it may be used to evaluate whether or not a model might walk well. To compare power for models of different sizes, we utilized standard techniques (given in Alexander, 1977; McMahon, 1984). The calculated powers were divided by the mass and the displacement of the centre of mass (CM) respectively so that the parameters might be compared directly. Further, since many muscles are involved in walking and each model will take a different period of time to complete a gait cycle, convenient comparison of the total effect of muscle parameters was facilitated by averaging the values of each muscle parameter over the cycle period to obtain the sum for that parameter. For example, the powers of a muscle at all instants during walking were firstly summed and divided by cycle time, then powers of all muscles were summed. This provides a simplified value for muscle power, which reflects the total effect of muscle power on a gait/speed combination. Though power may be greater or smaller in a muscle than in another, the average of all muscle powers may be a meaningful representation of that muscle's overall contribution to driving walking in a given model.

Results

The musculoskeletal model can be displayed as an animation sequence (movie available at http://www.liverpool.ac.uk/premog). The active state for any muscle/muscle group is shown by red colouring, and inactive as green. The ground reaction force (GRF) in the sagittal plane is represented as a black vector, the length indicating the magnitude of the GRF and the direction giving the orientation of the GRF (Fig. 3).

The calculated muscle parameters for AL 288-1 during normal walking are shown in Fig. 4,

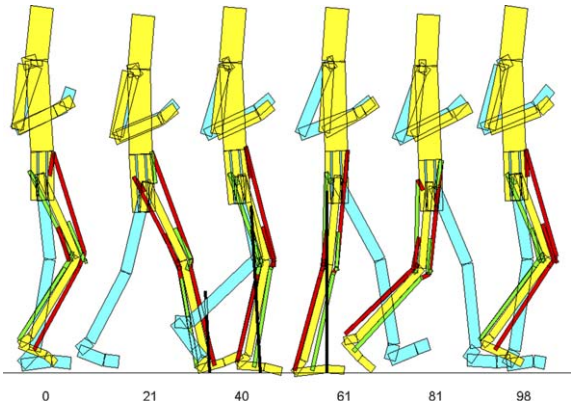

Fig. 3. Selected frames from a sequence of walking for the musculoskeletal model: X axis: percentage of a stride (heel strike at about 20% of the stride, toe off at about 80% of the stride); Black vectors represent ground reaction forces: the lengths scale to the magnitudes of the ground reaction force (GRF), and their direction gives the orientation of the GRF at that instant. The right leg includes 9 'muscle' groups, which are active in different phases of walking: red indicates that the muscle is active and green inactive (colours visible in animation available at http://www.liv.ac.uk/premog).

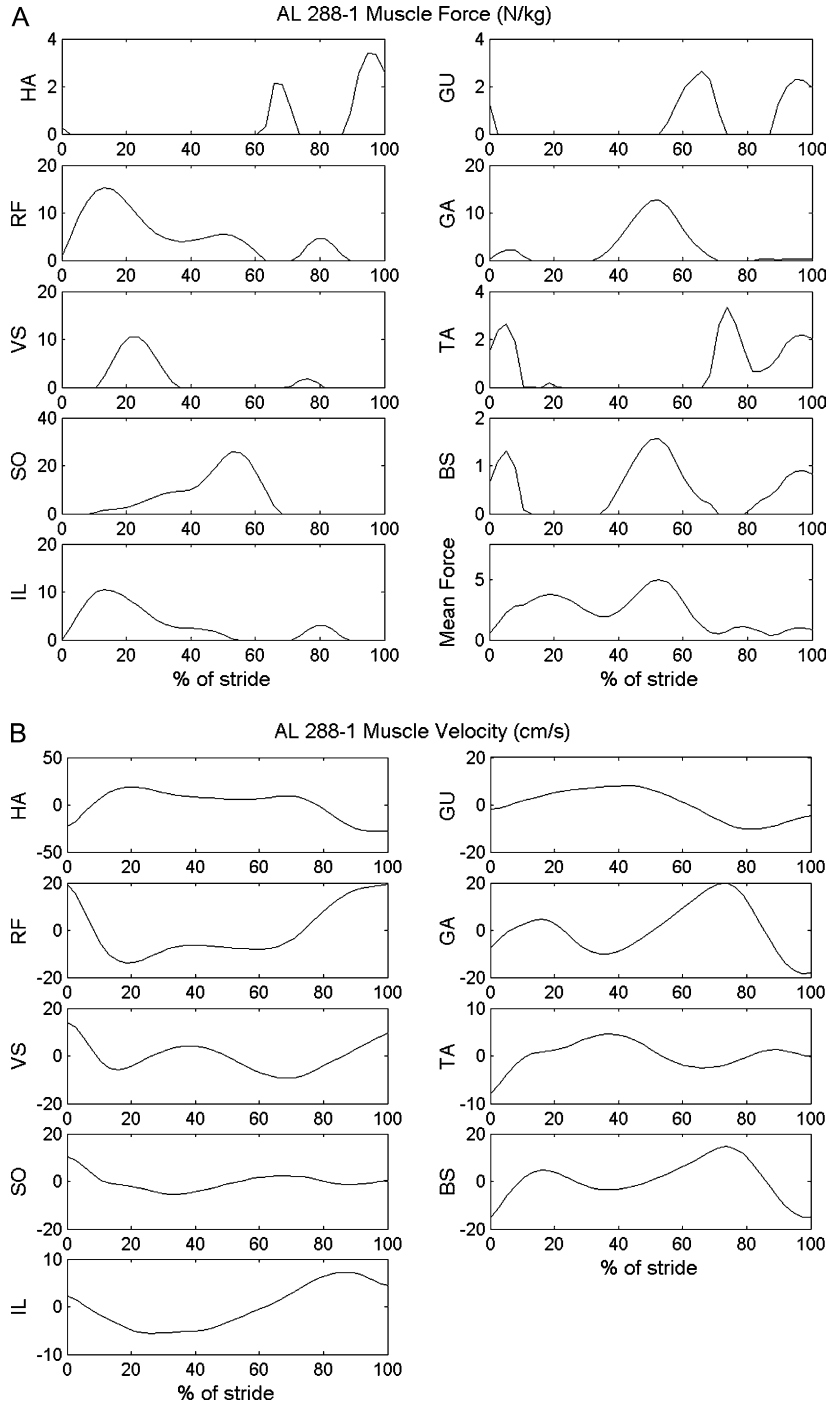

Fig. 4A. The calculated muscle force for the AL 288-1 model in normal walking. X axis: percentage of a stride, heel strike at about 0% of a stride, toe off at about 60% of a stride; Y axis: muscle force (N/kg) (RF: 'Rectus femoris'; VS: 'Medial and lateral vasti'; TA: 'Tibialis anterior'; GU: 'Gluteus maximus, medius and minimus'; HA: 'Semimembranosus and Semitendinosus'; GA: 'Gastrocnemius'; SO: 'Soleus'; BS: 'Biceps femoris, short head'; IL: 'Iliacus'. The last subplot (bottom, right) shows the average of all muscle forces.
Fig. 4B. Calculated muscle velocity in AL 288-1. Y: (cm/s). This figure shows the rate of shortening calculated for each 'muscle'. The rate of shortening has a low fluctuation compared to data for modern humans in Winter (1991).

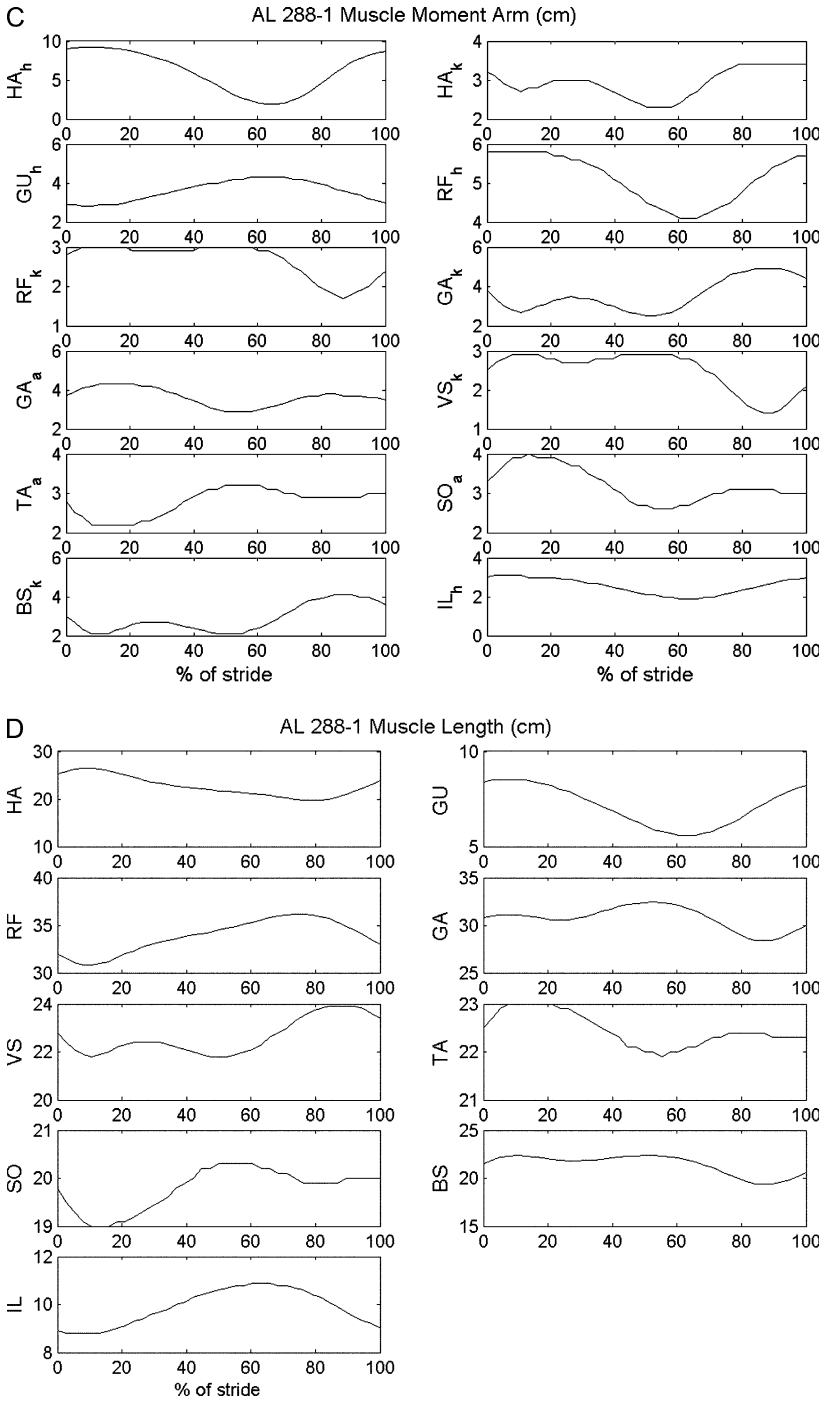

Fig. 4C. Calculated moment arms of muscle (MAM). Y: muscle names for MAM (cm), subscript: name of joint: h-hip, k-knee and a-ankle. A bi-articular muscle has two MAMs about two relative joints.

Fig. 4D. Calculated muscle length during normal walking in AL 288-1. Y(cm). This shows the length changes in muscle groups during walking, and by comparison with figures in Winter (1991) for modern humans indicates that AL 288-1 had relatively low fluctuations in muscle length.

including muscle forces, velocities, moment-arms and lengths.

All models were run through the same simulation in order to test their responses to different speeds or gaits. Limitations of space forbid showing all resulting charted data. Comparing the pattern of predicted muscle forces (Fig. 4A) to the pattern of EMG (Fig. 6) obtained from treadmill experiments on human walking shows that most of the muscle forces have similar tendencies to those for equivalent muscles in experimental records of EMG in Winter (1991) (for equivalents of SO, VS and GU) and Carey (1998) (for all others) if we apply, *pro tempore*, the reasonable activation delay. The curve for total muscle force has a form which from heel-strike to toe-off recalls the double-humped form of vertical GRFs obtained from force platform measurements, for normal upright walking at comfortable speed. Although we have not found any suggestion in the literature that this should be so, it is sensible to expect that muscle forces during walking should be proportional to the fluctuation in the external forces, such as GRFs.

Simulated muscle forces for KNM-WT 15000 are shown in Fig. 5 and averages of all muscle stresses were then obtained for the models (Fig. 7). The averages of all muscle powers were similarly obtained (see Fig. 8 and Table 6). As calculated powers have similar units (W/kg) as metabolic powers, predicted muscle powers are, for illustrative purposes, comparable with experimentally metabolic costs. Considering the efficiency of transfer of mechanical costs into physiological (metabolic) costs to be approximately 20-25% (Heglund and Cavagna, 1985), the calculated muscle parameters are in reasonable agreement with physiological experiments (see Table 6, see also Taylor et al., 1982).

Sensitivity studies

With a lower weight and shorter stature in comparison with modern humans, and long lever arms of muscles, our model predicts that AL 288-1 would have absolutely lower muscle stresses (N/cm^2) than either modern humans or

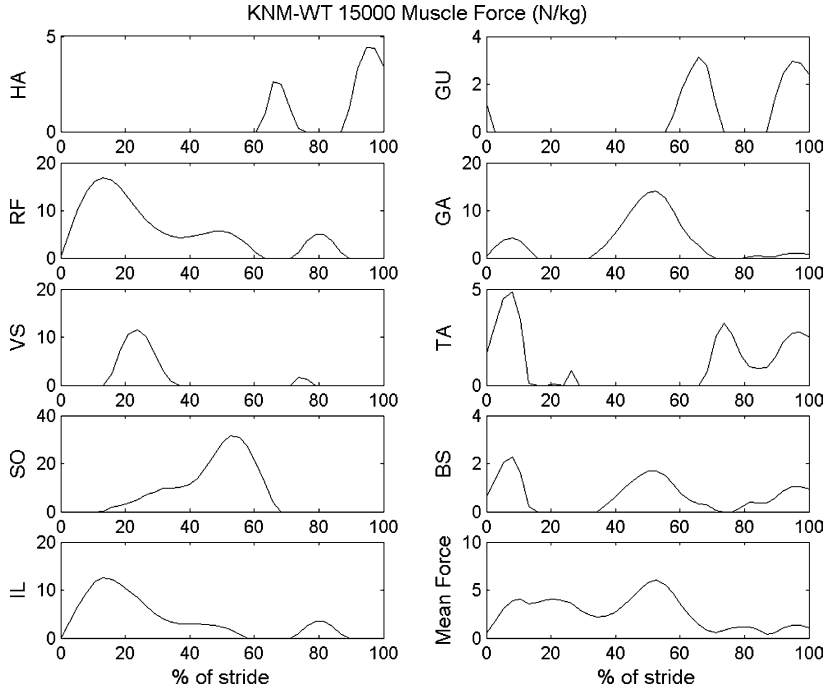

Fig. 5. Simulated muscle forces for KNM-WT 15000 in normal walking. The total mean of muscle forces (right bottom sub-figure) has a similar pattern to that of vertical ground reaction force recorded experimentally, from heel-strike (0%) to toe-off (60%).

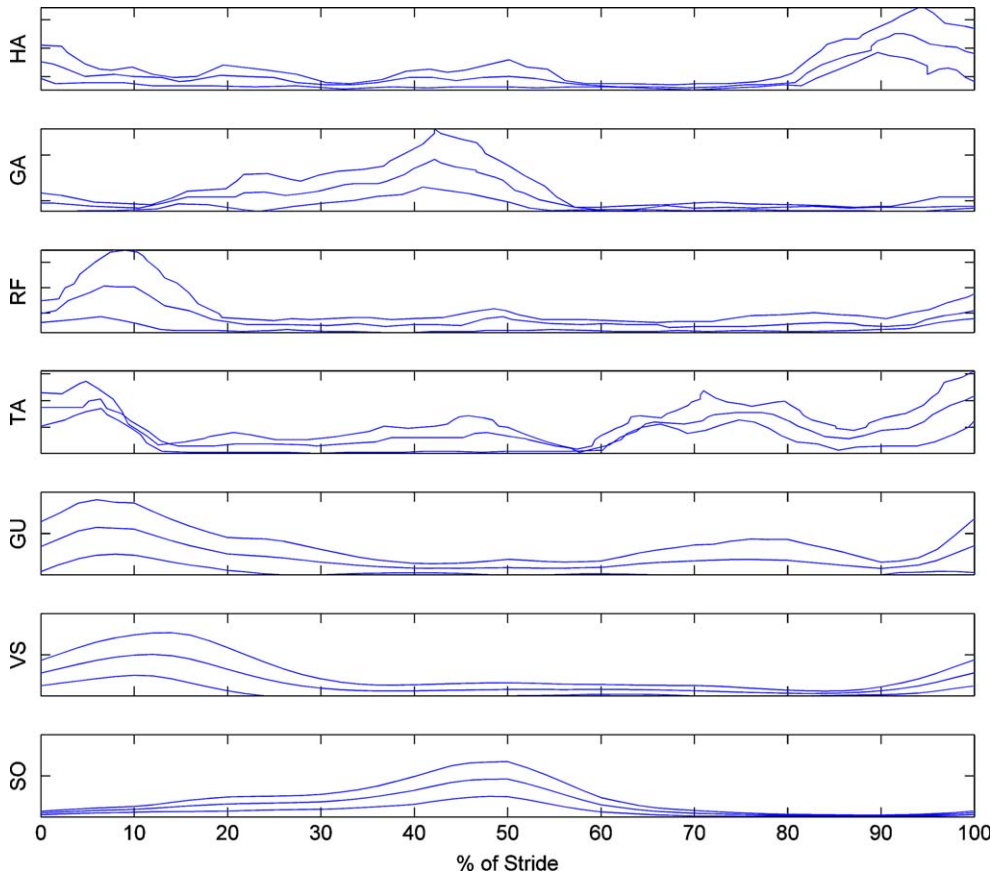

Fig. 6. EMG patterns of muscles corresponding to 'muscle' groups used in modeling. Those for HA, GA, TA and RF from Carey (1998), and others from Winter (1991). X: percent of a stride, heel strike at about 0% of a stride and toe off at about 60% of a stride; Y: arbitrary units.

KNM WT-15000 (see Fig. 7A): muscle stress, in AL 288-1, is about 60% that of other models (Fig. 8).

We also simulated BHBK walking by AL 288-1, with two alternative sets of PCSAs, one from chimpanzees and another from female humans, and the results are shown in Table 7. Muscle forces were again compared to EMG gathered by Carey (1998) during BHBK walking by humans and found to be a reasonable, though not perfect, match if a reasonable activation delay was taken into consideration (see Wang, 1999).

Inputting different lengths of the tibia to the model of AL 288-1 did not lead to significant change in the simulated results. Adjusting the crural index between 75 and 88 (tibia lengths 0.210 or 0.247 respectively), the maximum and minimum likely crural index for hominids (Aiello and Dean 1990; Richmond et al., 2002), simulated muscle parameters (e.g. the mean of muscle forces and the mean of absolute muscle powers) show only small differences (about 0.3%-0.7%) from those seen in the model for our chosen crural index value of 83.5/tibia length 0.235.

Neither did applying different body weights to the model of AL 288-1 bring significant changes. McHenry and Berger (1998) estimated weights for AL 288-1 within a range of 24-32 (kg). When we replaced the AL 288-1 model weight of 30 (kg) with 25 and 33 (kg), respectively, in normal walking gait, simulated muscle forces showed only small differences (0.09% and 0.2% N/kg greater)

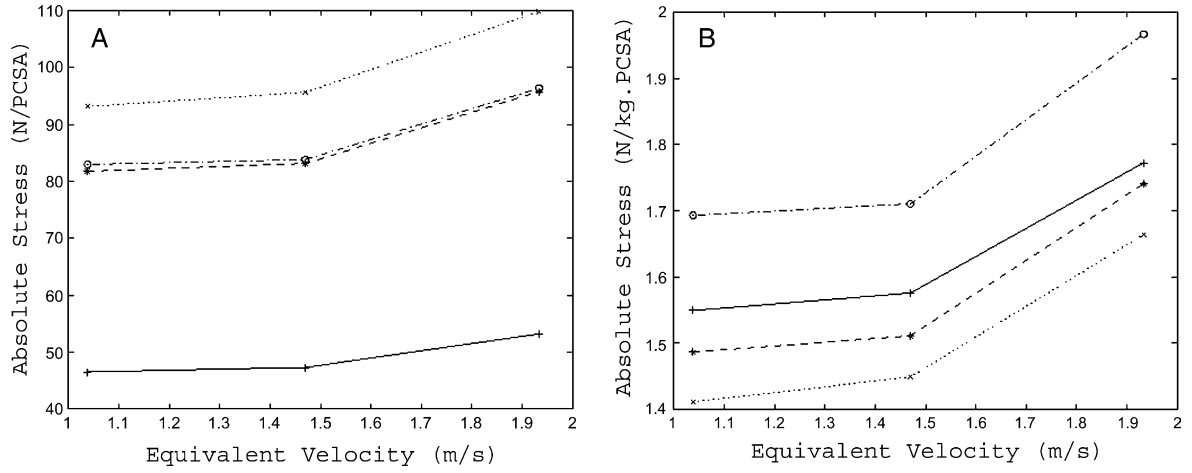

Fig. 7. Comparison of muscle stress for different models. A: muscle stress (N/cm^2); and B: muscle stress per unit of mass (N/kg.cm^{-2}). Solid line (+): AL 288-1; dashed and dotted line (o): KNM-WT15000; dashed line (*): Female1; and dotted line (x): Male1. The values of the equivalent velocities are from experimental results and shown for reference, and the actual velocities for the particular model depend on size and are listed in Table 5.

compared with the 30-kg model, as did simulated muscle power (W/kg) (0.06% and 0.14% greater respectively).

Attachments on the pelvis of the 'muscle' were varied over a reasonable range from their original position in both the anterior-posterior and superior-inferior directions. When RF attachments was moved 5% inferiorly, the total muscle force increased by 0.85% compared with moving 0.5% superiorly, and the total of muscle powers increased by 0.42% if moved inferiorly compared with movement superiorly, suggesting that muscle force and power are not very sensitive to inferior-superior displacement of muscle attachments. However, when the coordinates of RF's attachment were moved 5% of its coordinate

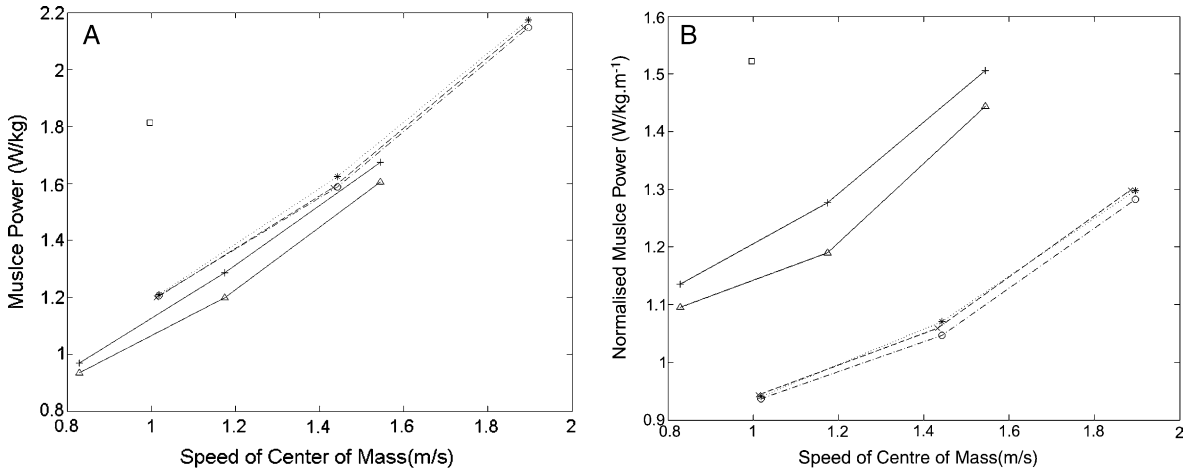

Fig. 8. Comparison of muscle power at various speeds for the different models. A: muscle power per unit of mass (W/kg); and B: muscle power per unit of mass and distance traveled (W/kg.m^{-1}). Solid line (+): AL 288-1 with human female PCSA at three speeds of erect walking; Solid line (Δ): AL 288-1 with chimpanzee PCSA at three speeds of erect walking; (□) AL 288-1 in BHBK gait; dashed and dotted line (o): KNM-WT15000; dashed line (*): Female1; and dotted line (x): Male1.

Table 6
Calculated Muscle Powers (W/kg) and Distance-specific Power ($W/kg.m^{-1}$)

Subjects	Slow	Normal	Fast	Slow	Normal	Fast
		(W/kg)			($W/kg.m^{-1}$)	
AL 288-1	0.9697	1.2856	1.6735	1.1355	1.2771	1.5060
KNM-WT 1500	1.2053	1.5876	2.1481	0.9367	1.0467	1.2828
Male1	1.2104	1.6232	2.1736	0.9406	1.0702	1.2980
Female1	1.1978	1.5851	2.1469	0.9431	1.0587	1.2990

Note: The results are in reasonable agreement with experimental metabolic data (Taylor et al., 1982): when the velocities vary from 0.5 to 2 (m/s), the mass-specific metabolic values are from 3.0 to 7.5 (W/kg).

anteriorly, the total of muscle forces decreased by 1.4% compared with when they were moved 5% posteriorly; and the total of muscle powers decreased by only 0.13% when moved anteriorly compared to posteriorly, implying that a different anterior-posterior position might benefit walking.

Discussion

Within the limits of technique and data, our results lead to the following considerations and tentative conclusions:

Comparison of power and metabolic costs

Positive and negative muscle powers may consume metabolic energy at different rates. It is not clear what the proportional relationship of the two forms is, although much effort has been directed to determining this relationship (e.g. Alexander, 1997; McMahon, 1984). In this study, therefore, both positive and negative powers are considered to make a contribution to total power requirements. It should be noted, however, that this study is not intended to predict metabolic costs from mechanical parameters, a task for which forwards dynamics is more appropriate. We have tried preliminary studies for humans and alternative gaits and builds in AL-288-1 (Sellers et al., 2003 and 2004). It is worth noting here that our finding that in the simulation of various gaits in AL 288-1 where PCSAs were assigned proportions typical of common chimpanzees required similar power to that in which PCSA proportions were taken from human females. This point needs to be verified by a further work.

Table 7
Calculated Muscle Parameters for the model of AL 288-1 in a 'bent-hip bent-knee' gait

	Power (W/kg)	Power/d ($W/kg.m^{-1}$)	Force (N/kg)	Stress (N/cm^2)	Stress/kg ($N/kg\ cm^{-2}$)
AL 288-1(C)	1.8132	1.5224	5.7330	51.0486	1.7016

Note: all parameters are represented by their averages; AL 288-1(C)'s PCSAs are normalized using chimpanzee data (Thorpe et al., 1999).

Comparison with EMG and force platform data

To evaluate our modelling results, we compared the pattern of predicted muscle forces to the pattern of EMG obtained from experiments on human walking. Abundant EMG data is available for humans from different sources (see e.g. Basmajian, 1974; Winter, 1991). Human data in Carey (1998) however are perhaps suitable for our purposes, as they were collected as part of an investigation of the gait of hominids. In comparison with the experimental recordings, and taking into consideration of the possible delay between muscle activation and force production, the curves of simulated muscle force for human walking are quite similar to experimental EMG (see Fig. 4A and Fig. 6); the same applied to comparisons of BHBK walking by the models and by humans (in Carey, 1998; compare Wang 1999). Thus, the modelling exercise may be regarded as a reasonably acceptable simulation, and its results therefore, also reasonably reliable. Unfortunately, such verification cannot with any confidence be extended beyond the human morphotype, as we have noted there is little EMG available for voluntary bipedalism of untrained, adult great apes other than humans.

Comparison of muscle stress

We found that muscle stress (N/cm^2) in AL 288-1, is about 60% that of other models. This

difference is certainly related to body size. AL 288-1 has a relatively heavy body mass, and thus relatively large PCSAs, which could decrease muscle stresses. Besides, it is likely to be related to body proportions: a consequence of relatively larger muscle moment arms. If we normalize muscle moment arms by leg length, we find that moment arms are 10% larger (Table 8) in the AL 288-1 model than in modern humans. Thus, to produce an equivalent moment of force at the joint, AL 288-1 is likely to exert a smaller muscle force. On the other hand, however, *muscle stresses per unit of mass* (N/kg.PCSA or N/kg.cm^2) are similar to, or even slightly greater in AL 288-1 than in modern humans (Fig. 7B), indicating that the body proportions of AL 288-1 may increase required muscle stress per unit of mass during walking.

In addition, KNM-WT 15000 is likely to have similar characteristics of muscle stress (N/cm^2) to humans (Fig. 7A), but the normalised stress (N/kg cm^2) in KNM-WT 15000 is slightly higher than other models (Fig. 7B), perhaps implying that its musculoskeletal proportions might not be as favourably configured as possible for effective use of muscle stress during human-like walking, although the body proportions of KNM-WT 15000 might benefit carrying-load walking (Wang and Crompton, 2004).

Comparison of muscle power

According to our results, AL 288-1 would use similar power (W/kg) in human-like upright walking as would our other models: the KNM-WT 15000 model, the human male and the human female (Fig. 8A and Table 6). There are two possible reasons for this: 1) AL 288-1 has relatively large muscle moment arms, as a consequence of segment proportions and bone shape; and 2) AL 288-1 had relatively small changes in muscle velocity and length (see Fig. 4B and D): which parameters are also affected by skeletal geometry.

Since the function of bipedal walking is of course to move the whole body over a distance, we need to consider the *power expenditure per unit of mass and per unit of displacement*, the distance-specific cost of transport. The distance-specific powers (W/kg.m^{-1}) are higher in AL 288-1 than in other models (Fig. 8B and Table 6), by 15%-20%. Those results indicate that the size and proportions of AL 288-1 may not have been beneficial to long distance bipedal walking, a suggestion previously made by Preuschoft and Witte (1991). In terms of power required for walking, however, KNM-WT 15000 seems to have similar effectiveness to modern humans (Fig. 8).

Table 8
Comparison of the normalised muscle parameters for different models.

	AL 288-1	KNM-WT 15000	Female1	Male1
MMF (N/kg)	2.2472	2.6116	2.6397	2.7981
MMV (m/s)	0.0626	0.0833	0.0814	0.0781
MMA (m)	0.0346	0.0457	0.0446	0.0428
MMA/LL (%)	6.77	5.94	5.86	5.56

Note: MMF is mean of muscle forces; MMV is mean of muscle velocities; MMA is the mean of all muscle moment arms; LL is leg length (see Table 1).

Model sensitivity

We found that the AL 288-1 model was not very sensitive to small changes in tibia length, and small errors in tibia length can thus probably safely be ignored. There is no indication, however, that large errors in proportions would be tolerable. Our finding may suggest that the model is unlikely to be sensitive to small differences in other lengths: but this was not the case for HAW, a stand-in for the triceps surae lever arm at the ankle joint, which suggests that mechanically key variables are likely to be much more sensitive. Inputting different lengths of the HAW to the model of AL 288-1 (see Table 1) did lead to significant changes in simulated results. If the foot of AL 288-1 were chimpanzee-like, the length would be about 21 cm (by comparison with measurements made from a chimpanzee of similar stature) and thus HAW about 1.8 (foot proportions taken from Schultz, 1963). In normal walking gait, the total of muscle forces is larger by 10.6% with a chimpanzee-like HAW than with human-like HAW, as might be

expected, because a smaller HAW lowers the moment arms of gastrocnemius and soleus. However, the total of muscle powers increases slightly more (0.7%) with a chimpanzee-like HAW than with a human-like HAW, indicating that gastrocnemius and soleus exert large forces while the muscle velocities are very slow. Sensitivity to length therefore needs testing in further, more systematic studies. With regarding to muscle attachment, the considerable effect which resulted when the origin of RF was moved 5% anteriorly underlines the power of our modelling technique to identify functional relationships which might otherwise have been overlooked.

Comparison with other models

Kramer and colleagues' theoretical model of AL 288-1 did not estimate muscle parameters, but analysed the external work done at different speeds, and suggested that AL 288-1's smaller dimensions reduces energy expenditure (Kramer, 1999; Kramer and Eck, 2000). However, they appear to have used a value of 0.265 (m) for the AL 288-1 tibia, implying a different measurement protocol than applied in this paper. That length would give a value of 95 for the crural index, which is outside a conservative range of 75-88 for humans and other living apes (Jungers, 1982; Aiello and Dean, 1990; Richmond et al., 2002).

To the extent that our model of the fossil species is reasonable accurate, the present study tends to lead to two possible conclusions: 1) considering mechanical power per unit of mass, the body proportions of AL 288-1 might require lower muscle stress during walking than those of *Homo* spp. (which might have facilitated adoption of habitual erect bipedal walking, rather than an expensive BHBK gait); *but* 2) considering power per unit mass *and* per unit displacement, the size and proportions of AL 288-1 might not have been suitable for bipedal walking over a long distance (and/or by extension at a high walking speed), implying that the musculoskeletal system of *Homo*, in contrast, might well be so adapted, as suggested in particular by Preuschoft and Witte (1991). This result is essentially in agreement with suggestions by Jungers (1982 and 1991) and McHenry (1991) that longer legs enable stride frequency to be reduced and hence save energy. Yamazaki et al. (1996) developed a neuro-musculo-skeletal model for the analysis of human evolution. Applying distance-specific power as a criterion, they concluded that rather larger size would be more energy-efficient than smaller size. We found that small changes in body weight, within the range suggested for AL 288-1 by McHenry (1991) exert only small influences on muscle force and power requirements. However, Kramer (1999) and Kramer and Eck (2000) argue, on the other hand, that AL 288-1 would have required lower mass specific power than modern humans though the cost of transport would be nearly identical. Our present findings suggest that power expenditure per unit of mass and per unit of displacement, the distance-specific cost of transport, was 15%-20% higher in AL 288-1 than in the KNM-WT 15000, and male and female human models. This in turn indicates that KNM-WT 15000 (and of course of modern humans) is better adapted for efficient long-distance or high-speed walking than AL 288-1. The proportions of the latter, however, by increasing moment arms, may have meant that it required absolutely lower muscle stress, which may possibly have eased the transition to terrestrial bipedalism.

Significance

This study thus suggests that (with the exception just remarked) lower or higher body mass does not of itself change the mechanical effectiveness of walking. This result echoes the comparison of metabolic costs of walking by human children and adults by Heglund and Schepens (2003). It is changing body proportions which exerts the stronger influence.

The evolution of bipedalism is of course likely to have involved many factors, environmental, dietary, and phylogenetic (Rose, 1991; Steudel, 1996; Richmond et al., 2001). The factors involved are unlikely to have remained the same, or equally influential, between the time when habitual terrestrial bipedalism first evolved, to that when endurant walking first developed. Early on, the absolutely

low muscle stresses made possible by large muscle moment arms (these in turn a consequence of short stature and short-legged, long-trunked limb proportions as well as bone geometry) may well have encouraged the transition to terrestrial bipedalism, perhaps by facilitating short bursts of speed and by helping muscles sustain upright posture. At a later stage the efficiency of long distance transport is likely to have become more important.

Aiello and Wheeler (1995) show that the proportions, and specifically the shorter trunk of early African *Homo ergaster*, as represented by KNM-WT 15000, suggests a higher-quality and less fibrous diet than that of *A. afarensis* (represented by AL 288-1) while Ruff (1991) and Wheeler (1992, 1993) point to the thermoregulatory advantages of the body proportions of early African *Homo ergaster*, particularly in the more xeric and open conditions apparently prevalent in East Africa at that time. Aiello and Wells (2002) suggest that a radically different foraging strategy, with a much greater content of animal protein, and use of body fat to buffer food scarcities in a more unstable environment, is implied by the new body form. Carrier (1984) has suggested that human body build enables us to be efficient endurance hunters: while we do find that high speed walking may be served by the changes in proportions from *Australopithecus* to *Homo*, the present study does not address the possibility of endurable running *per se*, since the energetic efficiency of human running relies on elastic storage of energy in connective tissue. However, it is likely that hunting-based selection for endurance would have affected both high and low speed pursuit capabilities. It is also worth bearing in mind that the morphological changes from *Australopithecus* to *Homo* which couple a shorter trunk with longer legs also serve to substantially increase the capacity to transport loads, both in the hand (Wang et al., 2003a) and over the shoulder or on the back (Wang and Crompton, 2004). Lithic evidence is our most direct source of evidence of transport. For Olduwan industries, transport of tools or raw materials over distances of 3km – 12 km have been established (Leakey 1971; Hay 1976); East Turkana also provides instances of the importation of raw material onto flood plains of the ancient lake, over distances of up to 20 km. (Harris and Herbich 1978). However, in Acheulean sites, evidence suggests that transport occurs more often — and over much greater distances. At Gadeb, in eastern Ethiopia, dated at about 1.5 MYA, several obsidian bifaces apparently document a transport distance of over 100 km. (Clark, 1980). The latter is of course contemporaneous with early African *Homo ergaster*. Is this a coincidence? Possibly, but we think not. The mechanical response of the new, short-trunked long-legged morphology is thus likely to have been selected for in part by the demands of increased transport, as well as of ranging distance and other factors such as those indicated above.

Summary

This study built an inverse-dynamics musculoskeletal model of the lower limb for early hominids and modern humans, capable of estimating the patterns of muscle force during bipedal walking. Skeletal dimensions were derived from the literature (for AL 288-1) or by measurement of a cast (for KNM-WT 15000). Relative muscle attachments typical of modern humans were applied to the models. Joint motion and moments from the experiments on humans walking were input into the models, to permit calculation of muscle stress and power. The calculated muscle forces were compared with the EMG from experiments. The performance of the models was examined in several modes of erect walking and in a 'bent-hip bent-knee' gait. The results show that: 1) evaluated by power expenditure per unit of mass in walking (W/kg), AL 288-1 would have similar power requirements to those of modern humans; but, 2) with distance-specific parameters as criteria, this early hominid would expend relatively more power ($W/kg.m^{-1}$) than *Homo*, tentatively suggesting (subject to the limitations of our model) that in the evolution of bipedalism, hominid body proportions have evolved so as to obtain an effective application of muscles to bipedal walking over a long distance (or, possibly, and not necessarily contemporaneously, at high speed).

Acknowledgements

This research has been supported by grants from the Biotechnology and Biological Sciences Research Council, the Natural Environment Research Council, and The Leverhulme Trust, UK. The authors thank the Associate Editor and the three Referees for constructive comments during peer-review.

Appendix

A substantial body of data were available for use in this study from our own experiments on human walking (Wang, 1999). Kinematic and kinetic data used in this study are derived from 6 subjects (statures 1.6-1.8 m, weights 56-82 kg) who were required to walk upright at three self-determined speeds: slow, normal, fast (averages 1.03, 1.47 and 1.93 m/s), and to simulate "bent-hip bent-knee" walking (at circa 1.23 m/s). Synchronized 250 Hz 4-camera digital video was recorded together with ground reaction forces, from a Kistler force platform. The necessary data: joint angles and moments, were derived from these recordings using specially written software (Wang, 1999). When compared with other authors (Winter, 1991; Eng and Winter 1995), the joint angles and moments (see Figs. A1-2) show similar pattern and magnitude. The differences are likely to derive from selected walking speeds, joint marker positions, and the filter parameters for smoothing raw data. Since our own joint angles and moments were both used for the models, the input data (joint angles and moments), the output data (the

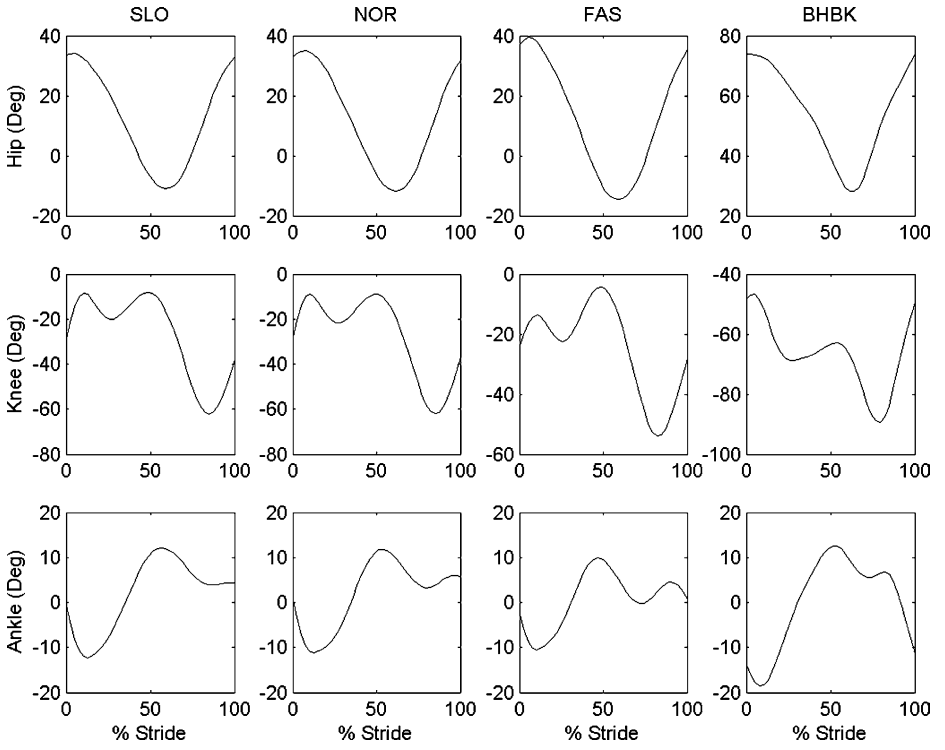

Fig. A1. The joint angles for four gaits. Erect modes of walking at slow speed (SLO), normal speed (NOR), and fast speed (FAS), and 'bent-hip bent-knee' walking (BHBK). Each column represents a gait and each row joint angles for that gait. Heel strike occurs at about 0% of the stride and toe off at about 60% of the stride. With the addition of data in the Tables on the models used, and joint moments, given in Fig A2, this gives inputs required to duplicate our experiments.

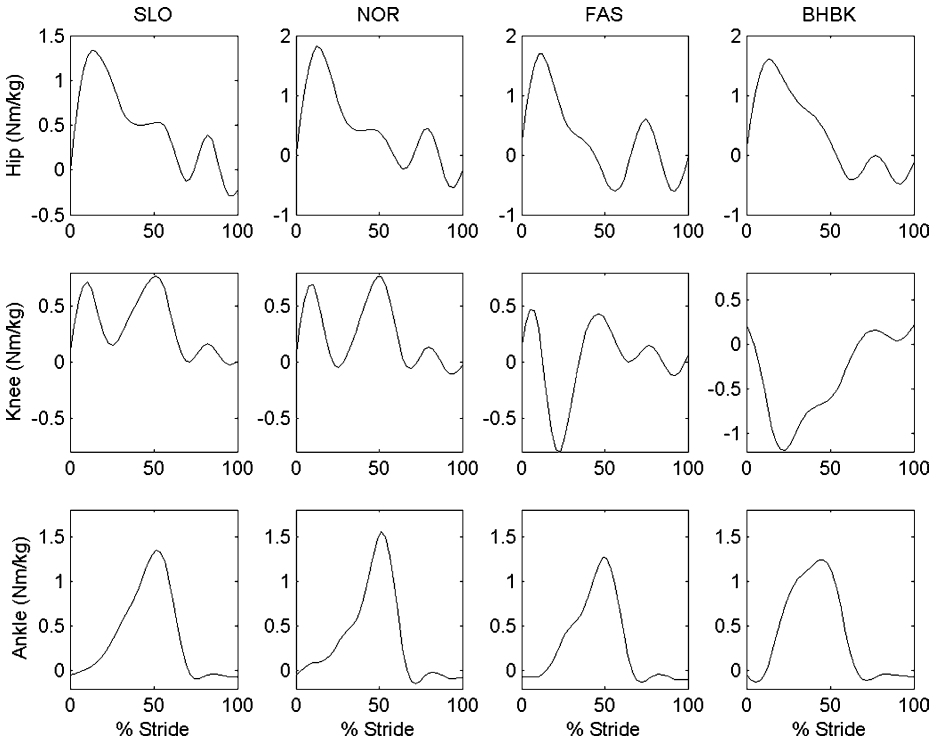

Fig. A2. The joint moments for four gaits. Each row represents the joint moment (Nm/kg) for that gait. Erect modes of walking at slow speed (SLO), normal speed (NOR), and fast speed (FAS), and in 'bent-hip bent-knee'(BHBK) walking. Heel strike occurs at about 0% of the stride and toe off at about 60% of the stride. With the addition of data in the Tables on the models used, and joint angles, given in Fig A1, this gives inputs required to duplicate our experiments.

muscle parameters), and the analysis (e.g. power) in this study are internally consistent.

References

Aiello, L., Dean, C., 1990. An Introduction to Human Evolutionary Anatomy. Academic Press, London, pp. 249.

Aiello, L.C., Wheeler, P., 1995. The expensive tissue hypothesis: the brain and digestive system in human and primate evolution. Curr. Anthropol. 36, 199–221.

Aiello, L.C., Wells, J.C.K., 2002. Energetics and the evolution of the genus *Homo*. Annu. Rev. Anthropol. 31, 323–338.

Alexander, R.McN., 1977. Terrestrial locomotion. In: Alexander, R.McN., Goldspink, G. (Eds.), Mechanics and Energetics of Animal Locomotion. Chapman and Hall, London, pp. 168–201.

Alexander, R.McN., 1984. Stride length and speed for adults, children and fossil hominids. Am. J. Phys. Anthropol. 63, 23–27.

Alexander, R.McN., 1985. The maximum forces exerted by animals. J. Exp. Biol. 115 (1), 231–238.

Alexander, R.McN., 1992. Mechanics of animal locomotion (in Advances in Comparative and Environmental Physiology 11). Springer-Verlag, London.

Alexander, R.McN., 1997. Optimum muscle design for oscillatory movements. J. Theo. Biol. 184, 253–259.

Basmajian, J.V., 1974. Muscle alive, their functions revealed by electromyography, third ed. Williams and Wilkins Co, Baltimore.

Biewener, A.A., 1989. Scaling body support in mammals- limb posture and muscle mechanics. Science 245 (4913), 45–48.

Brown, F., Harris, J., Leakey, R., Walker, A., 1985. Early *Homo erectus* skeleton from west Lake Turkana, Kenya. Nature 316, 788–792.

Carey, T.S., 1998. The energetics of "bent-knee, bent-hip" walking in humans: implications for the evolution of bipedalism in early hominids. Ph.D Thesis, the University of Liverpool.

Carrier, D.R., 1984. The energetic paradox of human running and hominid evolution. Curr. Anthropol. 25 (4), 483–495.

Clark, J.D., 1980. The Plio–Pleistocene environmental and cultural sequence at Gadeb, northern Bale, Ethiopia. In: Leakey, R.E., Ogot, B. (Eds.), Proceedings of the 7th

Panafrican Congress of Prehistory and Quaternary Studies. TILLMIAP, Nairobi, pp. 89–93.

Crompton, R.H., Li, Y., Alexander, R.McN., Wang, W.J., Günther, M.M., 1996. Segment inertial properties of primates: new techniques for laboratory and field studies of locomotion. Am. J. Phys. Anthropol. 99 (4), 547–570.

Crompton, R.H., Li, Y., Wang, W.J., Gunther, M.M., Savage, R., 1998. The mechanical effectiveness of erect and "bent-knee, bent-hip" bipedal walking in *Australopithecus afarensis*. J. Hum. Evol. 35, 55–74.

Crompton, R.H., Thorpe, S., Wang, W.J., Li, Y., Payne, R., Savage, R., Carey, T., Aerts, P., Van Elsacker, L., Hofstetter, A., Gunther, M., Richardson, J., 2003. The biomechanical evolution of erect bipedality. Cour. Forsch.-Inst. Senckenberg 243, 135–146.

Crowninshield, R.D., Brand, R.A., 1981. A physiological based criterion of muscle force prediction in locomotion. J. Biomech. 14, 793–801.

Eng, J.J., Winter, D.A., 1995. Kinetic analysis of the lower limbs during walking: what information can be gained from a three-dimensional model? J. Biomech. 28, 753–758.

Friederich, J.A., Brand, R.A., 1990. Muscle fibre architecture in the human lower limb. J. Biomech. 23, 91–95.

Gillis, G.B., Biewener, A.A., 2002. Effects of surface grade on proximal hindlimb muscle strain and activation during rat locomotion. J. Appl. Physiol. 93, 1731–1743.

Glitsch, U., Baumann, W., 1997. The three-dimensional determination of internal loads in the lower extremity. J. Biomech. 30, 1123–1131.

Hardt, D.E., 1978. Determining muscle forces in the leg during normal human walking- an application and evolution of optimization methods. J. Biomech. Eng. 100, 74–78.

Harris, J.W.K., Herbich, L., 1978. Aspects of early Pleistocene hominid behaviour east of Lake Turkana, Kenya. In: Bishop, W.W. (Ed.), Geological Background to Fossil Man. Geol. Soc. London/Scottish Academic Press, Edinburgh, pp. 529–548.

Hase, K., Yamazaki, N., 2002. Computer simulation study of human locomotion with a three-dimensional entire-body neuro-musculo-skeletal model (I. Acquisition of normal walking). JSME Int. J. Ser. C-Mech. Syst. Machine Elements Manufact. 45, 1040–1050.

Hatze, H., 1977. A complete set of control equations for the musculoskeletal system. J. Biomech. 10, 799–805.

Hay, R.L., 1976. Geology of the Olduvai Gorge. University of California Press, California.

Heglund, N.C., Cavagna, G.A., 1985. Efficiency of vertebrate locomotory muscles. J. Exp. Biol. 115, 283–292.

Heglund, N.C., Schepens, B., 2003. Ontogeny recapitulates physloeny? Locomotion in children and other primitive hominids. In: Bels, V.L., Gasc, J.-P., Casinos, A. (Eds.), Vertebrate Biomechanics and Evolution. BIOS Scientific Publishers, Oxford, pp. 283–295.

Hill, A.V., 1938. The heat of shortening and dynamic constants of muscle. Proc. R. Soc. B 126, 136–195.

Hill, A.V., 1950. The dimensions of animals and their muscular dynamics. Science Progr. 38, 209–230.

Hof, A.L., Berg, J.V.D., 1981. EMG to force processing I: an electrical analogue of the Hill muscle model. J. Biomech. 14, 747–758.

Johanson, D.C., Lovejoy, C.O., Kimbel, W.H., White, T.D., Ward, S.C., Bush, M.E., Latimer, B.M., Coppens, Y., 1982. Morphology of the Pliocene Partial hominid skeleton (AL 288-1) from the Hadar formation, Ethiopia. Am. J. Phys. Anthropol. 57, 403–452.

Jungers, W.L., 1982. Lucy's limbs: skeletal allometry and locomotion in *Australopitbecus afarensis*. Nature 297, 676–678.

Jungers, W.L., 1991. A pygmy perspective on body size and shape in *Australopithecus afarensis* (AL 288-1, 'Lucy'). In: Coppens, Y., Senut, B. (Eds.), Origines de la Bipedie chez les Hominides. Editions du CRNS, Paris, pp. 215–224.

Kimbel, W.H., Johanson, D.C., Rak, Y., 1994. The first skull and other new discoveries of *Australopithecus afarensis* at Hadar, Ethiopia. Nature 368, 449–451.

Kimura, T., Okada, M., Ishida, H., 1979. Kinesiological characteristics of primate walking: its significance in human walking. In: Morbeck, M.E., Preuschoft, H., Gomberg, N. (Eds.), Environment, Behaviour and Morphology: Dynamic Interactions in Primates. Gustav Fischer, New York, pp. 297–311.

Kramer, P.A., 1999. Modeling the locomotor energetics of extinct hominids. J. Exp. Bio. 202, 2807–2818.

Kramer, P.A., Eck, G.G., 2000. Locomotor energetics and leg length in hominid bipedality. J. Hum. Evol. 38, 651–666.

Leakey, M.D., 1971. Olduvai Gorge, Vol. III: Excavations in Beds I and 11, 1960–1963. Cambridge University Press, Cambridge.

Li, Y., Crompton, R.H., Alexander, R.McN., Gunther, M.M., Wang, W.J., 1996. Characteristics of ground reaction forces in normal and chimpanzee-like bipedal walking by humans. Folia Primatol. 66, 137–159.

Lovejoy, C.O., 1981. The origin of man. Science 211, 341–350.

Matlab® 2002. The software for mathematical analysis. Matlab is a trademark of MathWorks, Inc.

McHenry, H.M., Berger, L.R., 1998. Body proportions in *Australopithecus afarensis* and *A. africanus* and the origin of the genus *Homo*. J. Hum. Evol. 35, 1–22.

McHenry, H.M., 1991. Femoral lengths and stature in Plio-Pleistocene hominids. Am. J. Phys. Anthropol. 85, 149–158.

McMahon, T.A., 1984. Muscles, Reflexes and Locomotion. Princeton University Press, Princeton, New Jersey.

Neptune, R.R., Kaute, S.A., Zajac, F.E., 2001. Contributions of individual ankle plantar flexors to support, forward progression and swing initiation during normal walking. J. Biomech. 34, 1387–1398.

Olney, S.J., Winter, D.A., 1985. Prediction of knee and ankle moments of force in walking from EMG and kinematic data. J. Biomech. 18, 9–20.

Oxnard, C.E., Crompton, R.H., Liebermann, S.S., 1989. Animal Lifestyles and Anatomies: The Case of the Prosimian Primates. Washington University Press, Seattle, pp. 174.

Patriarco, A.G., Mann, R.W., Simons, S.R., Mansourss, J.M., 1981. An evaluation of the approaches of optimization models in the prediction of muscle forces during human gait. J. Biomech. 14, 513–525.

Pedotti, A., Krishnan, V.V, Stark, L., 1978. Optimization of muscle-force sequencing in human locomotion. Math. Biosci. 38, 57–76.

Preuschoft, H., Witte, H., 1991. Biomechanical reasons for the evolution of hominid body shape. In: Coppens, Y., Senut, B. (Eds.), Origines De La Bipedie Chez Les Hominides (Cahiers de Paleoanthropologie). Editions du CNRS, Paris.

Prost, J.H., 1980. Origin of bipedalism. Am. J. Phys. Anthropol. 52, 175–189.

Richmond, B.G., Begun, D.R., Strait, D.S., 2001. Origin of human bipedalism: The knuckle-walking hypothesis revisited. Yrbk. Phys. Anthropol. 44, 70–105.

Richmond, B.G., Aiello, C.A., Wood, B.A., 2002. Early hominin limb proportions. J. Hum. Evol. 43, 529–548.

Rose, M.D., 1991. The process of bipedalization in hominids. In: Coppens, Y., Senut, B. (Eds.), Origine(s) de la bipedie chez les hominids. CNRS, Paris, pp. 37–48.

Ruff, C.B., 1991. Climate and body shape in hominid evolution. J. Hum. Evol. 21, 81–105.

Schultz, A.H., 1963. The relative lengths of the foot skeleton and its main parts in primates. Symp. Zool. Soc. Lond. 1, 199–206.

Seireg, A., Arvikar, R.J., 1973. A mathematical model for evaluation of forces in lower extremities of the musculoskeletal system. J. Biomech. 6, 313–326.

Sellers, W.I., Dennis, L.A., Crompton, R.H., 2003. Predicting the metabolic energy costs of bipedalism using evolutionary robotics. J. Exp. Biol. 206, 1127–1136.

Sellers, W.I., Dennis, L.A., Wang, W.J., Crompton, R.H., 2004. Evaluating alternative gait strategies using evolutionary robotics. J. Anat. 204, 343–351.

Steudel, K., 1996. Limb morphology, bipedal gait, and the energetics of hominid locomotion. Am. J. Phys. Anthropol. 99, 345–355.

Stern, J.T., Susman, R.L., 1983. The locomotor anatomy of *Australopithecus afarensis*. Am. J. Phys. Anthropol. 60, 279–317.

Susman, R.L., Stern, J.T., Jungers, W.L., 1984. Arboreality and bipedality in the Hadar hominids. Folia Primatol. 43, 113–156.

Taylor, C.R., Heglund, N.C., Malory, G.M., 1982. Energetics and mechanics of terrestrial locomotion. J. Exp. Biol. 97, 1–21.

Thorpe, S.K., Li, Y., Crompton, R.H., Alexander, R.McN., 1998. Stresses in human leg muscles in running and jumping determined by force plate analysis and from published magnetic resonance Imaging. J. Exp. Biol. 201, 63–70.

Thorpe, S.K.S., Crompton, R.H., Gunther, M.M., Ker, R.F., Alexander, R.M., 1999. Dimensions and moment arms of the hind- and forelimb muscles of common chimpanzees (*Pan troglodytes*). Am. J. Phys. Anthrop. 110, 179–199.

Wang, W.J., Crompton, R.H., Li, Y., Gunther, M.M., 1996. Comparison of the powers at the lower limb joints during walking at different velocities and their significance for a possible optimal walking velocity. In: Hakke, S. (Ed.), The Engineering of Sport 1. Balkema, Rotterdam, pp. 71–75.

Wang, W.J., Crompton, R.H., Wood, C.G., Li, Y., Günther, M.M., 1998. The concept of positive and negative signs for work, power and energy and their special meaning in biomechanics. In: Hakke, S. (Ed.), The Engineering of Sport 2. Blackwell, London, pp. 225–232.

Wang, W.J., 1999. The mechanics of bipedalism in relation to load-carrying: biomechanical optima in hominid evolution. Ph.D Thesis, the University of Liverpool.

Wang, W.J., Crompton, R.H., Li, Y., Gunther, M.M., 2003a. Optimum ratio of upper to lower limb lengths in hand-carrying of a load under the assumption of frequency coordination. J. Biomech. 36, 249–252.

Wang, W.J., Crompton, R.H., Li, Y., Gunther, M.M., 2003b. Energy transformation during erect and 'bent-hip, bent-knee' walking by humans with implications for the evolution of bipedalism. J. Hum. Evol. 44, 563–579.

Wang, W.J., Crompton, R.H., 2003. Size and power required for motion with implications for the evolution of early hominids. J. Biomech. 36, 1237–1246.

Wang, W.J., Crompton, R.H., 2004. The role of load-carrying in the evolution of modern skeletal proportions. J. Anat. 204, 417–430.

Ward, C.V., 2002. Interpreting the posture and locomotion of *Australopithecus afarensis*: where do we stand? Yrbk. Phys. Anthropol. 45, 185–215.

Webb, D., 1996. Maximum walking speed and lower limb length in hominids. Am. J. Phys. Anthropol. 101, 515–525.

Wheeler, P.E., 1992. The thermoregulatory advantages of large body size for hominids foraging in savanna environments. J. Hum. Evol. 23, 351–362.

Wheeler, P.E., 1993. The influence of stature and body form on hominid energy and water budgets: a comparison of *Australopithecus* and early *Homo*. J. Hum. Evol. 24, 13–28.

Wickiewicz, T.L., Roy, R.R., Powell, P.L., Edgerton, V.R., 1983. Muscle architecture of the human lower limb. Clin Orthop. Rel. Res. 179, 275–283.

Winter, D.A., 1990. Biomechanics and Motor Control of Human Movement. John Wiley and Sons, Inc., New York.

Winter, D.A., 1991. The Biomechanics and Motor Control of Human Gait: Normal, Elderly and Pathological, second ed. University of Waterloo Press, Canada.

Wolpoff, M.H., 1983. Lucy's lower limbs: long enough for Lucy to be fully bipedal? Nature 304, 59–61.

Yamazaki, N., Hase, K., Ogihara, N., Hayamizu, N., 1996. Biomechanical analysis of the development of human bipedal walking by a neuro-musculo-skeletal model. Folia Primatol. 66, 253–271.